



the  
**abdus salam**  
international centre for theoretical physics

SMR: 1133/2

**WINTER COLLEGE ON  
SPECTROSCOPY AND APPLICATIONS**

( 8 - 26 February 1999)

---

**"X-UV Spectroscopy with Synchrotron Radiation"**

presented by:

**Massimo ALTARELLI**

Abdus Salam ICTP

Trieste, Italy

and

Sincrotrone Trieste

Padriciano, 99

Trieste, Italy

---

These are preliminary lecture notes, intended only for distribution to participants.

strada costiera, 11 - 34014 trieste italy - tel. +39 40 2240111 fax +39 40 224163 - sci\_info@ictp.trieste.it - www.ictp.trieste.it



# VUV and X-ray Spectroscopy

1. Introduction to Synchrotron Radiation Sources
2. Photoemission (UPS, XPS, ARPES)
3. Absorption Spectroscopies (XANES, EXAFS, Dichroism)

Phys. Rev. 71, 829 (1947)

## Radiation from Electrons in a Synchrotron

F. R. ELDER, A. M. GUREWITSCH, R. V. LANGMUIR,  
AND H. C. POLLOCK

*Research Laboratory, General Electric Company,  
Schenectady, New York*

May 7, 1947

HIGH energy electrons which are subjected to large accelerations normal to their velocity should radiate electromagnetic energy.<sup>1-4</sup> The radiation from electrons in a betatron or synchrotron should be emitted in a narrow cone tangent to the electron orbit, and its spectrum should extend into the visible region. This radiation has now been observed visually in the General Electric 70-Mev synchrotron.<sup>5</sup> This machine has an electron orbit radius of 29.3 cm and a peak magnetic field of 8100 gausses. The radiation is seen as a small spot of brilliant white light by an observer looking into the vacuum tube tangent to the orbit and toward the approaching electrons. The light is quite bright when the x-ray output of the machine at 70 Mev is 50 roentgens per minute at one meter from the target and can still be observed in daylight at outputs as low as 0.1 roentgen.

The synchrotron x-ray beam is obtained by turning off the r-f accelerating resonator and permitting subsequent changes in the field of the magnet to change the electron orbit radius so as to contract or expand the beam to suitable targets. If the electrons are contracted to a target at successively higher energies, the intensity of the light radiation is observed to increase rapidly with electron energy.

## Maxwell's Equations:

$$\operatorname{div} \vec{E} = 4\pi \rho$$

$$\operatorname{div} \vec{B} = 0$$

$$\operatorname{curl} \vec{E} = -\frac{1}{c} \frac{\partial \vec{B}}{\partial t}$$

$$\operatorname{curl} \vec{B} = \frac{4\pi}{c} \vec{j} + \frac{1}{c} \frac{\partial \vec{E}}{\partial t}$$

$\vec{E}$  = electric field

$\vec{B}$  = magnetic induction

c = speed of light

$\vec{j}$  = current density

$\rho$  = charge density

$$\operatorname{div} \vec{A} = \frac{\partial}{\partial x} A_x + \frac{\partial}{\partial y} A_y + \frac{\partial}{\partial z} A_z$$

$$(\operatorname{curl} \vec{A})_x = \frac{\partial}{\partial y} A_z - \frac{\partial}{\partial z} A_y$$

y } by circular perm. x, y, z.

## Radiation of accelerated charges.

Larmor's formula :

$$P = \frac{2e^2}{3c^3} |\vec{v}|^2 \quad (|\vec{v}| \ll c)$$

Total radiated power (energy per unit time of electromagnetic waves created) by particle of charge  $e$ , subject to acceleration

$$\vec{v} \equiv \frac{d\vec{r}}{dt}$$

Examples of accelerated motion:

\* Simple harmonic motion

$$x = x_0 \sin \omega t \quad \dot{x} = \omega x_0 \cos \omega t = v_x \\ \ddot{x}_x = -\omega^2 x_0 \sin \omega t$$

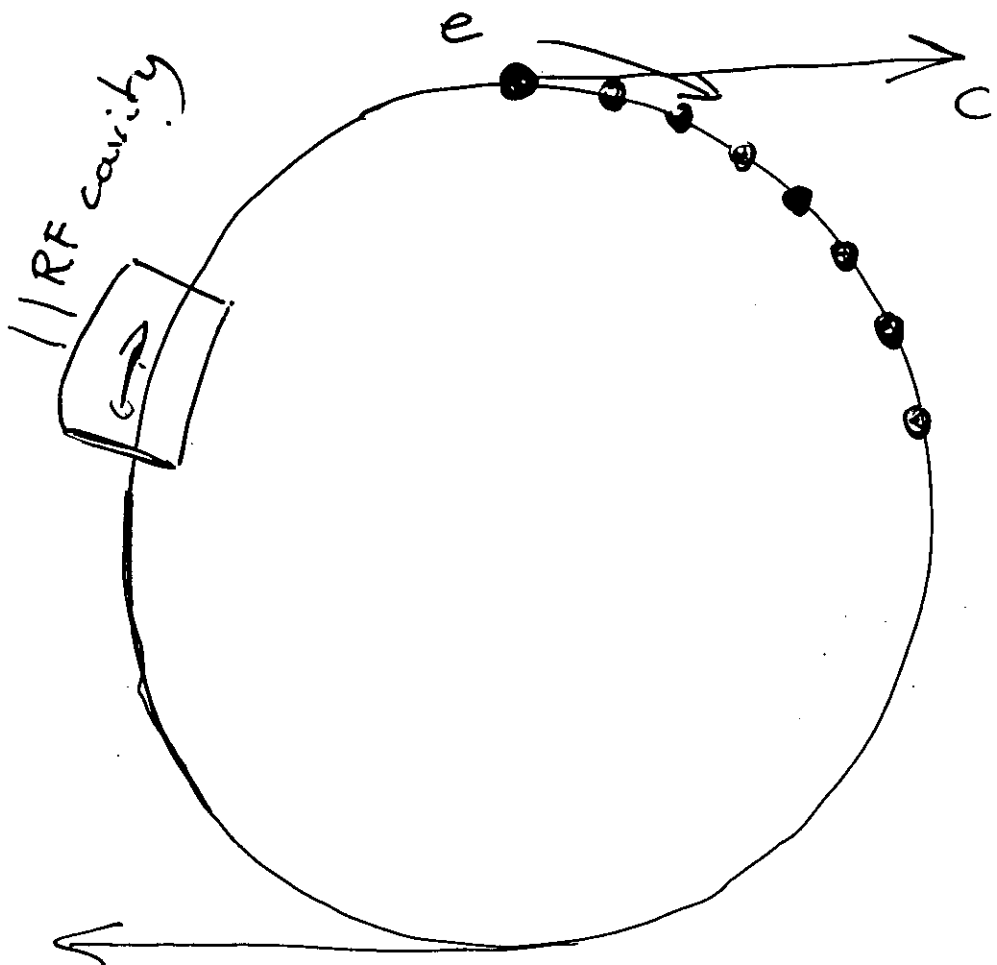


\* Circular motion

$$|\vec{v}| = \frac{v^2}{r} = \omega^2 r$$



# Application to Circular Accelerator.



$$E = \gamma m_0 c^2 = \frac{m_0 c^2}{\sqrt{1 - \beta^2}}$$

- Electrons or Positrons  $m_0 c^2 = 511 \text{ keV} \approx 0.5 \text{ MeV}$
- Protons  $m_0 c^2 \approx 1 \text{ GeV}$

So a 1 GeV  $e^-$  ring has

$$\gamma \sim 2 \times 10^3$$

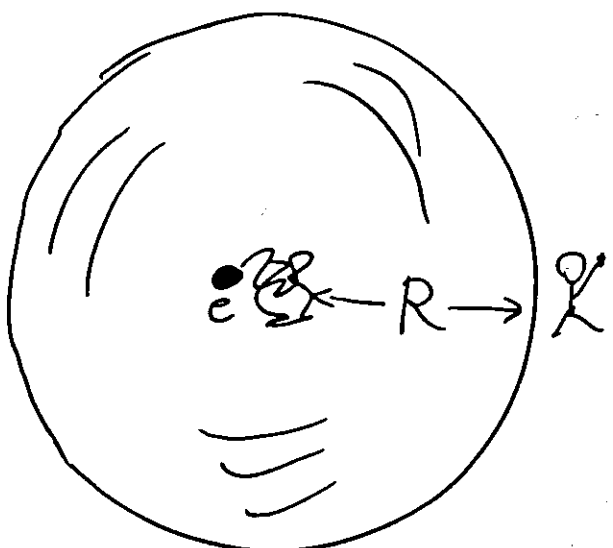
Relativistic generalization:  
for  $|\vec{v}|$  not so smaller than c.

Lienard formula (1898)

$$P = \frac{2}{3} \frac{e^2}{c^3} \gamma^6 \left( |\vec{v}|_{\text{ret}}^2 - \left| \frac{\vec{v} \times \vec{v}}{c} \right|_{\text{ret}}^2 \right)$$

$$= \frac{2}{3} \frac{e^2}{c} \gamma^6 \left( |\vec{\beta}|_{\text{ret}}^2 - \left| \vec{\beta} \times \vec{\beta} \right|_{\text{ret}}^2 \right)$$

"ret" means retarded, i.e. evaluated at time  $t - R/c$ ,  $R$ : distance of charge to observer



$$\vec{\beta} = \frac{\vec{v}}{c}$$

$$\gamma = \frac{1}{\sqrt{1 - \beta^2}}$$

$$E = \frac{m_0 c^2}{\sqrt{1 - \beta^2}} = \gamma m_0 c^2$$

Circular Geometry:

$$\vec{\beta} \perp \dot{\vec{\beta}} \Rightarrow |\vec{\beta} \times \dot{\vec{\beta}}|^2 = \dot{\beta}^2 \ddot{\beta}^2$$

$$P = \frac{2}{3} \frac{e^2}{c} \gamma^6 \left( \dot{\beta}^2 - \dot{\beta}^2 \ddot{\beta}^2 \right) = \\ = \frac{2}{3} \frac{e^2}{c} \gamma^6 (1 - \dot{\beta}^2) \dot{\beta}^2 = \frac{2}{3} \frac{e^2}{c^3} \gamma^4 \dot{v}^2$$

$$|\dot{v}| = \frac{c^2}{R}, \quad \dot{v}^2 = \frac{c^4}{R^2}$$

$$P = \frac{2}{3} \frac{e^2 c}{R^2} \gamma^4$$

Energy lost by  $e^-$  to radiation  
in one turn:

time for one turn

$$\Delta t = \frac{2\pi R}{\beta c} \sim \frac{2\pi R}{c}$$

(usually:  
 $\sim \mu\text{sec}'$ )

$$\delta E \equiv P \cdot \Delta t = \frac{4\pi}{3} \frac{e^2}{R} \gamma^4$$

Put numbers:

$$|| \quad \delta E (\text{in MeV}) = 0.0885$$

$$\left[ \frac{E (\text{in GeV})}{R (\text{in m})} \right]^4$$

ESRF:  $E = 6 \text{ GeV}$

$R = 25 \text{ m}$

$$\delta E = (0.0885 \cdot \frac{6^4}{25}) \text{ MeV}$$

$$= 4.6 \text{ MeV}$$

Electrons loose all energy in  $< 10^{-2} \text{ sec!}$

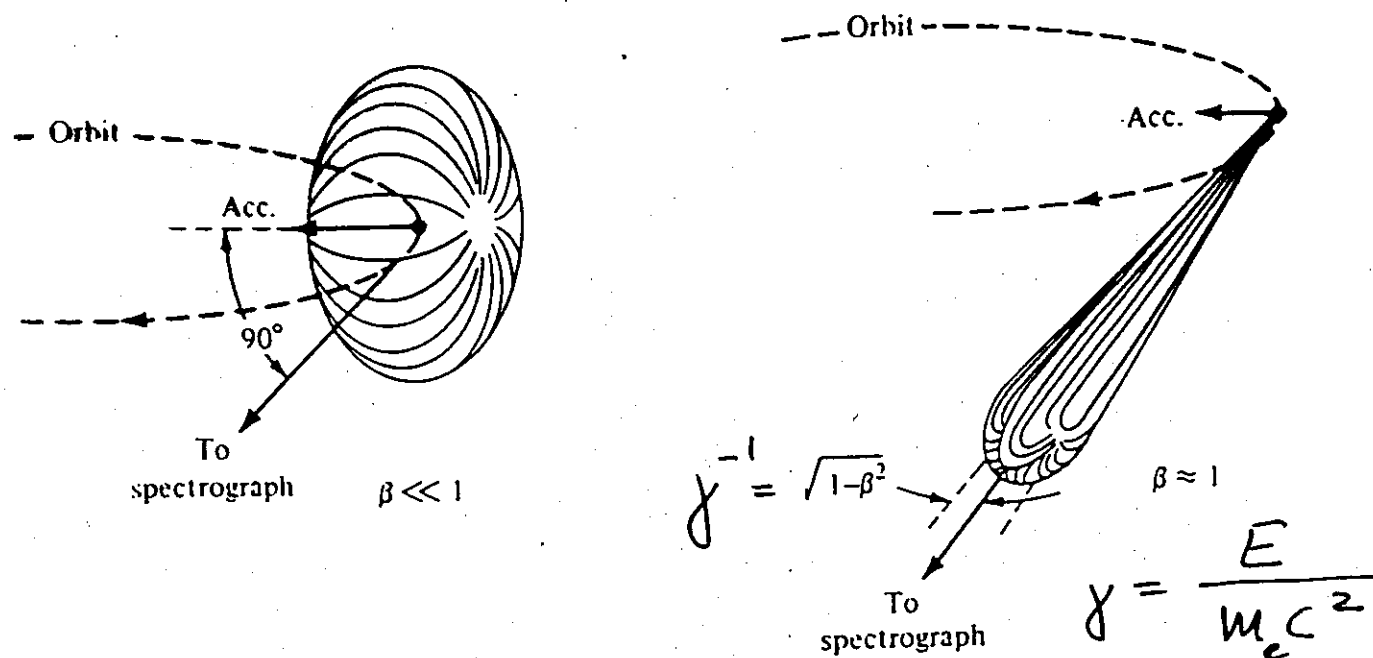
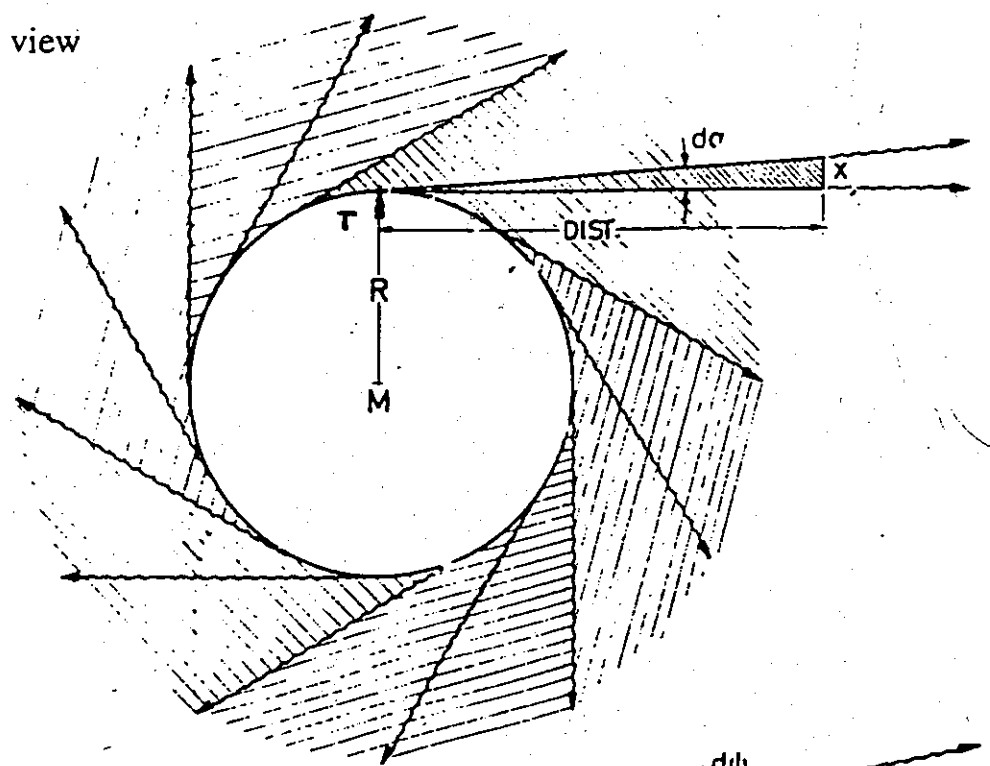
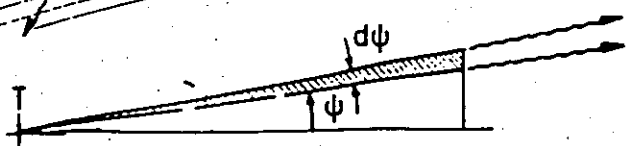


Fig. 5a. The "classical" picture for the geometry of synchrotron radiation emission (from Tomboulian and Hartman (1956)). The angular distribution (dipole pattern) of emitted intensity from a slow electron on a circular orbit (left) is distorted into a narrow cone in the instantaneous direction of motion for a relativistic electron moving with a velocity close to that of light ( $\beta = v/c = 1$ ) (right).

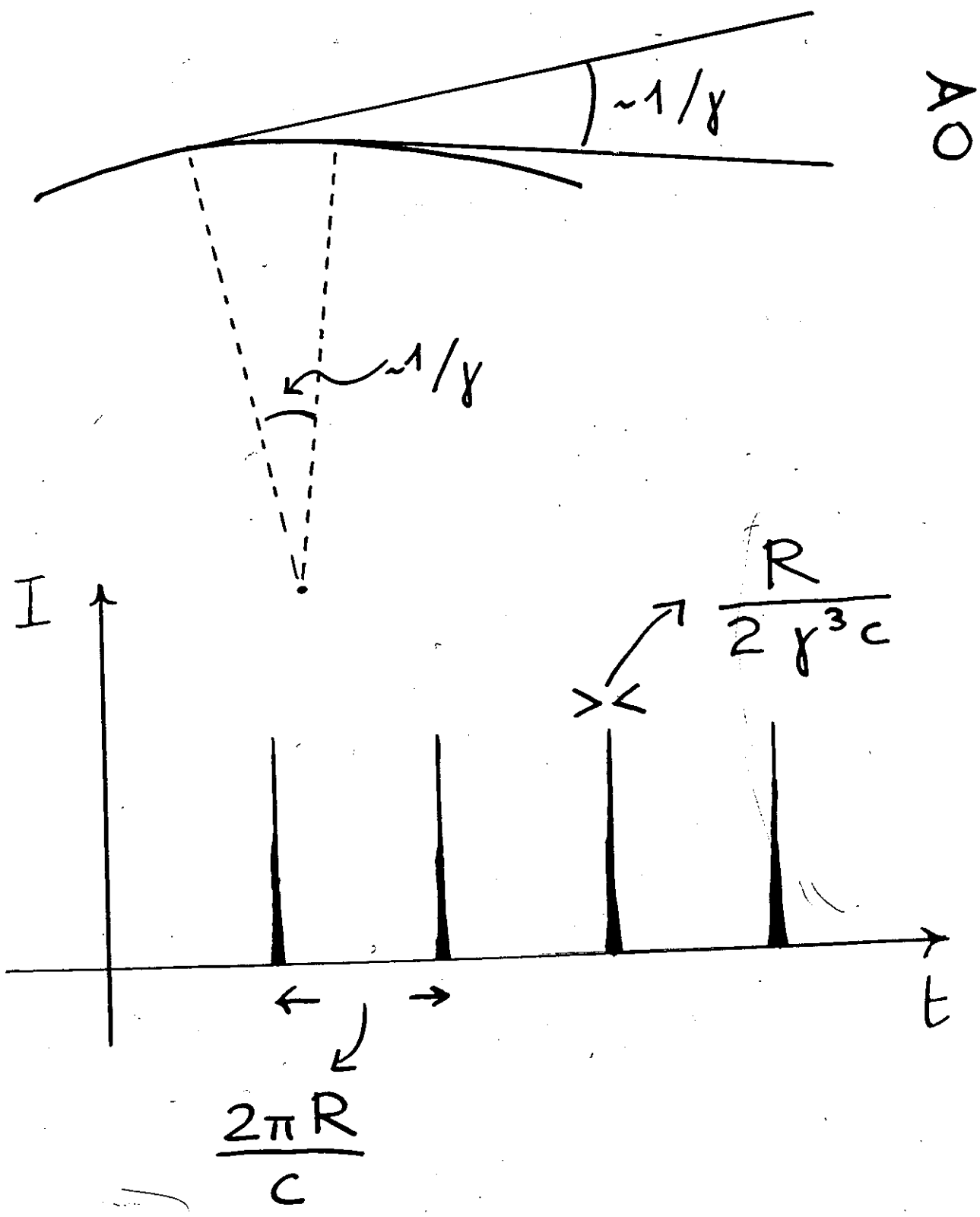
Top view



Side view



# Frequency distribution



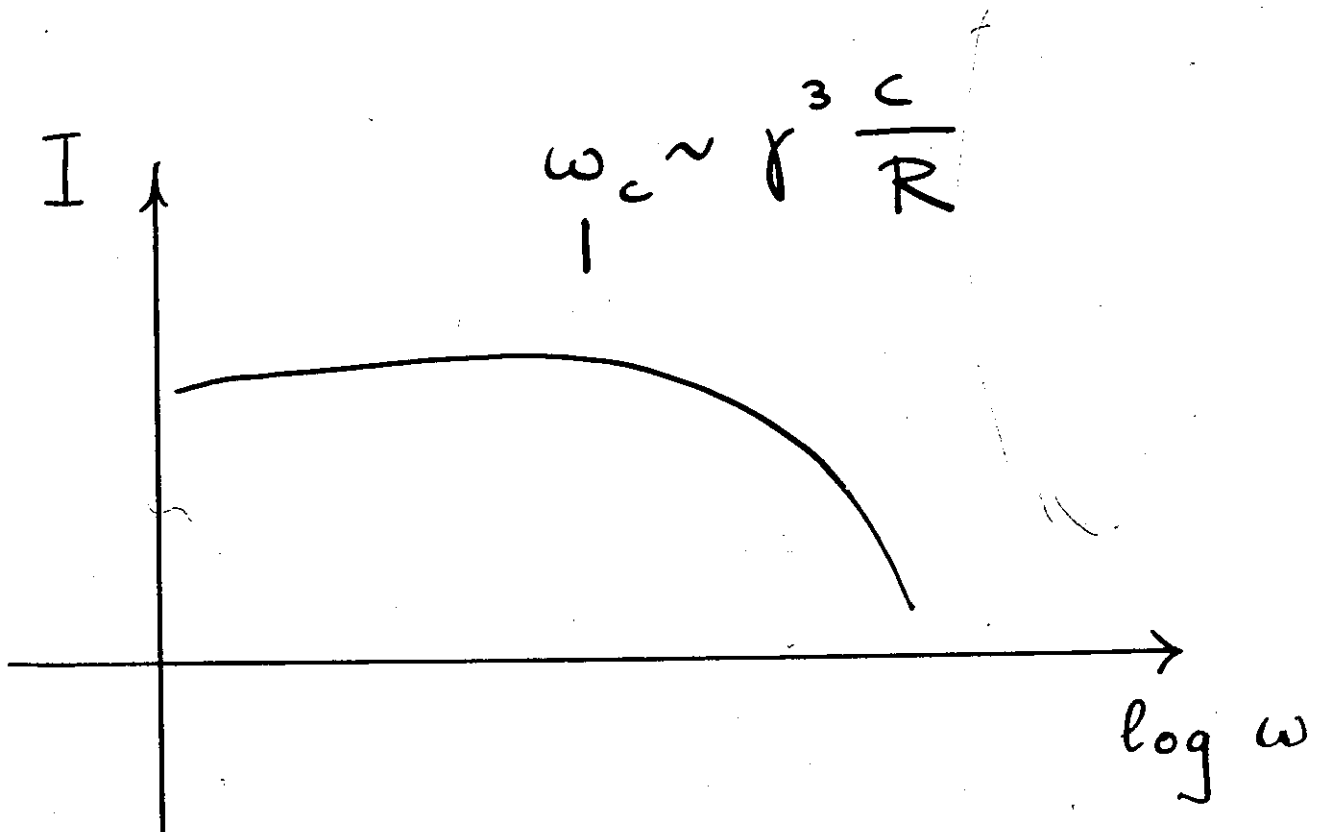
Broad (white) spectrum

from

$$\omega_0 \sim \frac{c}{2\pi R} \quad (\text{MHz})$$

to at least

$$\omega_c \sim r^3 \frac{c}{R} \quad (\sim 10^{10} - 10^{12} \omega_0)$$



More precisely:

Critical frequency:

$$\omega_c = \frac{3}{2} r^3 \frac{c}{R}$$

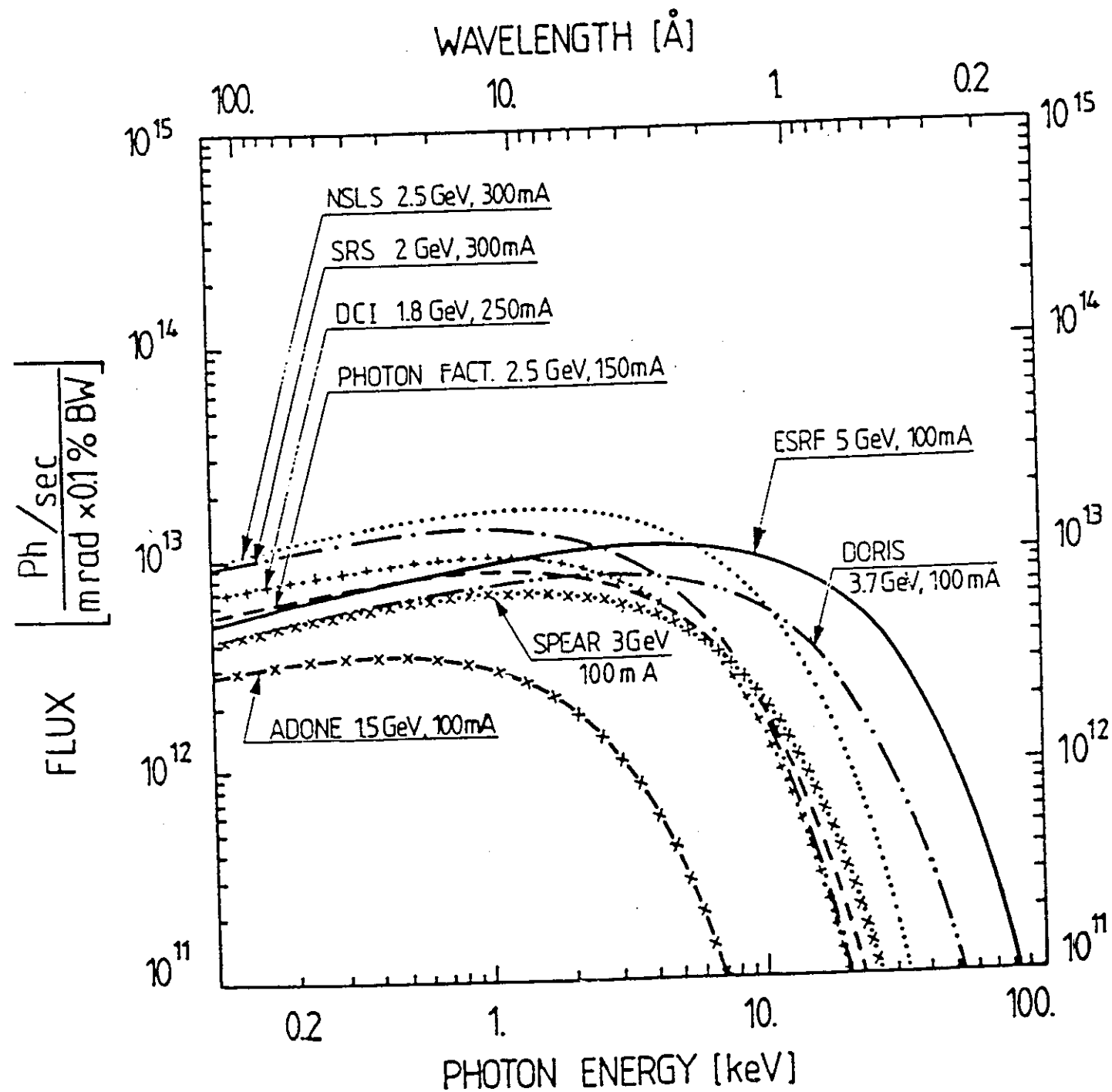
Half power emitted at  $\omega < \omega_c$

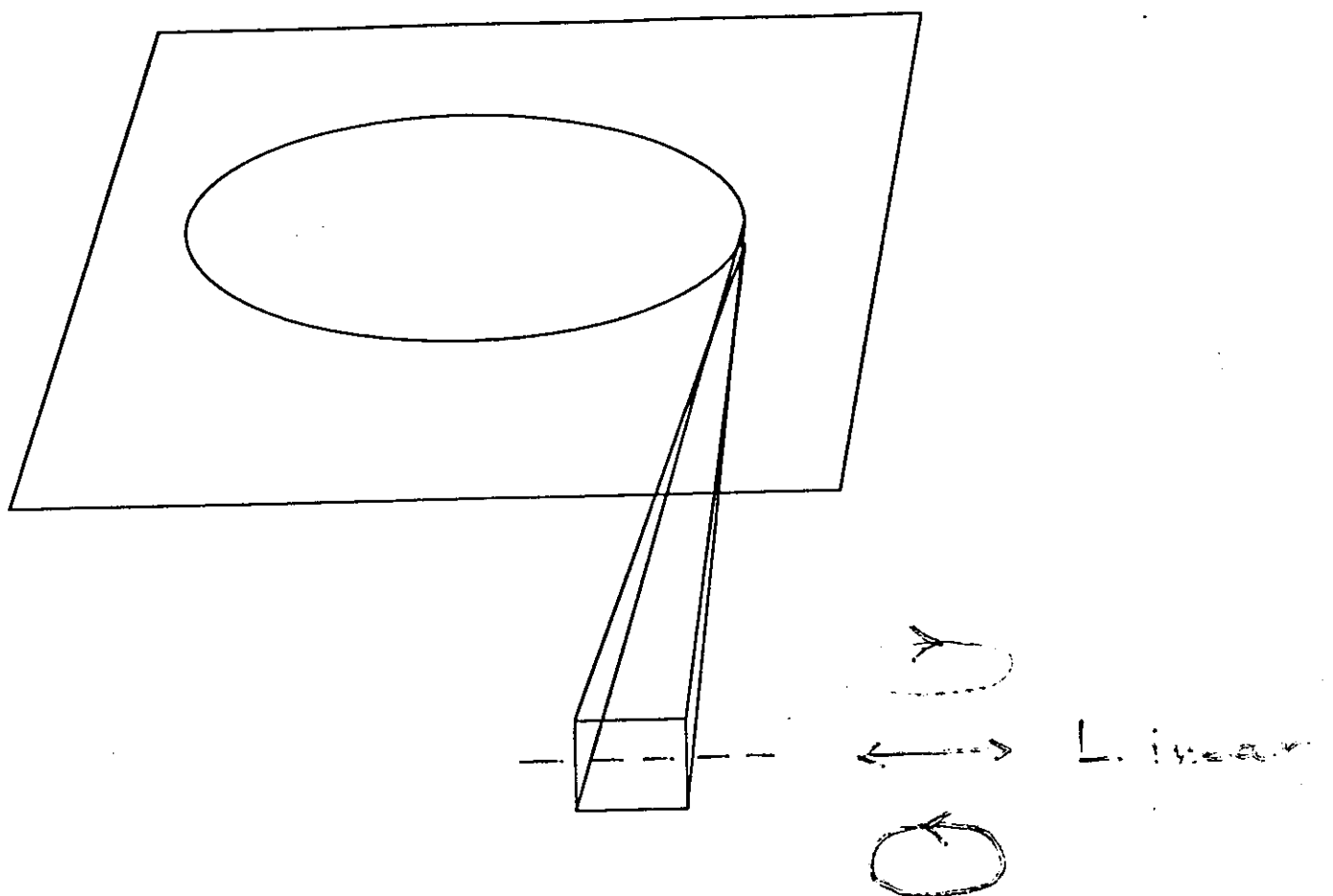
" " " "  $\omega > \omega_c$

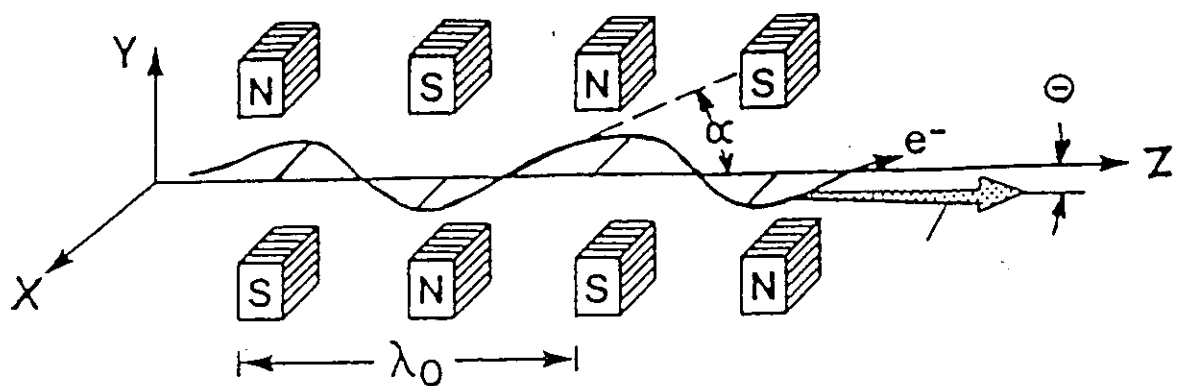
$$\omega_c \sim \omega_c \chi^3$$

$$\chi = \frac{E}{m_e c^2}$$

$$m_e c^2 = 0.511 \text{ MeV}$$





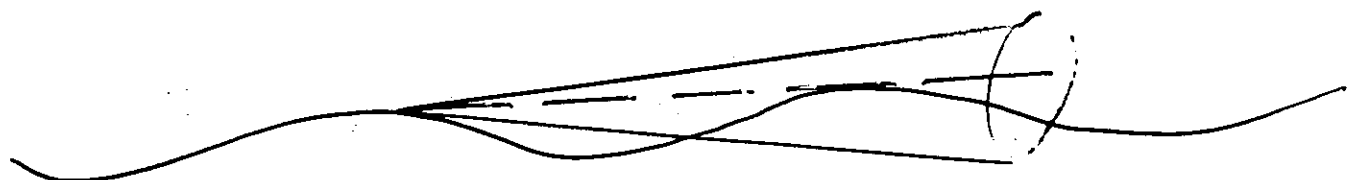
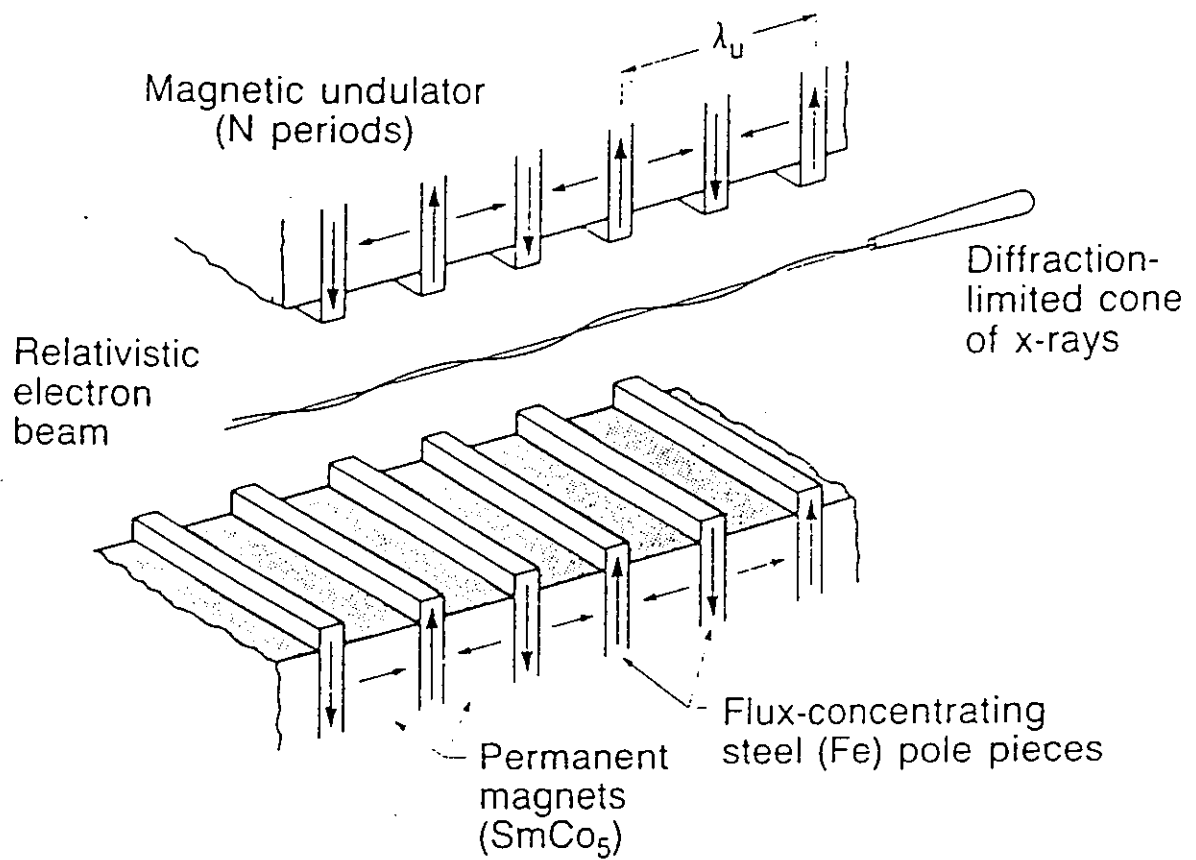


## Insertion Devices

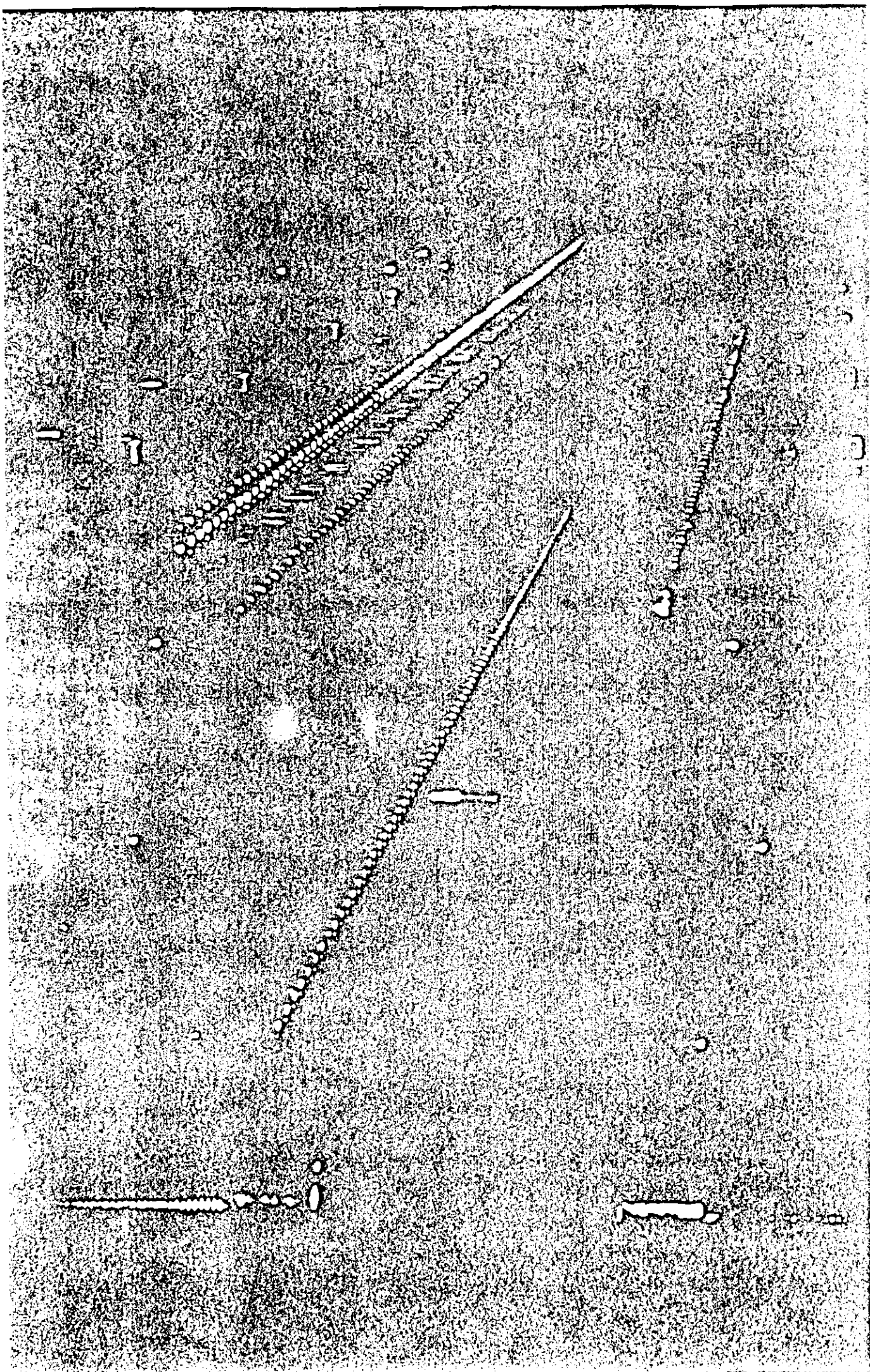
$$K = 93.4 \lambda_0 [m] B_0 (T)$$

$$K = \alpha \cdot \gamma = \alpha \frac{1}{\sqrt{1 - v^2/c^2}} \lesssim 1 \text{ Undulators}$$

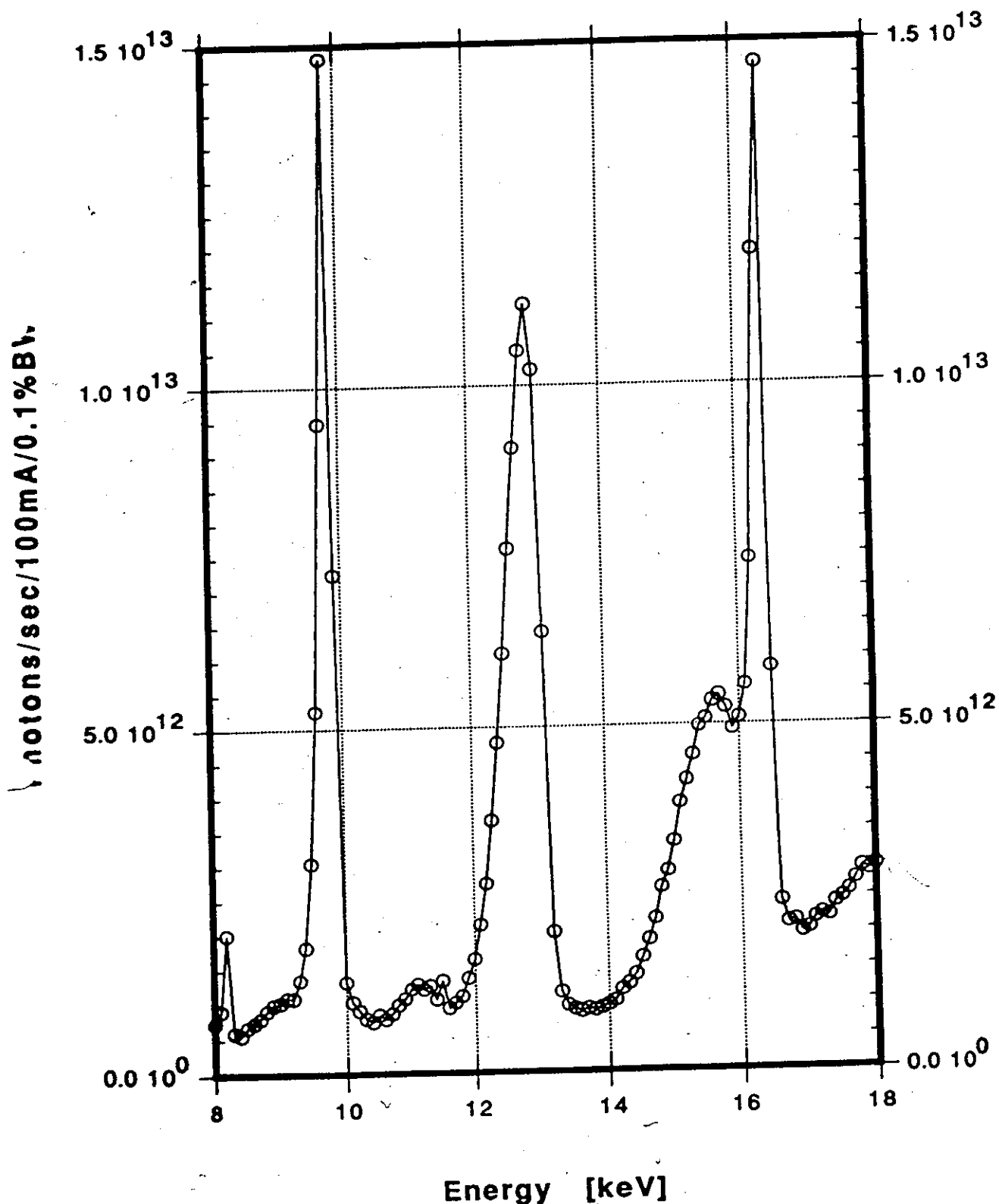
$\gg 1$  Wigglers



$$\text{electron delay} = n \lambda$$



**ID10 Undulator Spectrum at 22.8 mm Gap**  
**Si(220) Monochromator at 28.5m from source**  
**Primary Slits: 0.4mm(v), 0.5mm(h)**  
**(measured with NaJ(Tl) and calib. Kapton foil,**  
**corrected for absorption)**



# Undulator Emission

On Axis

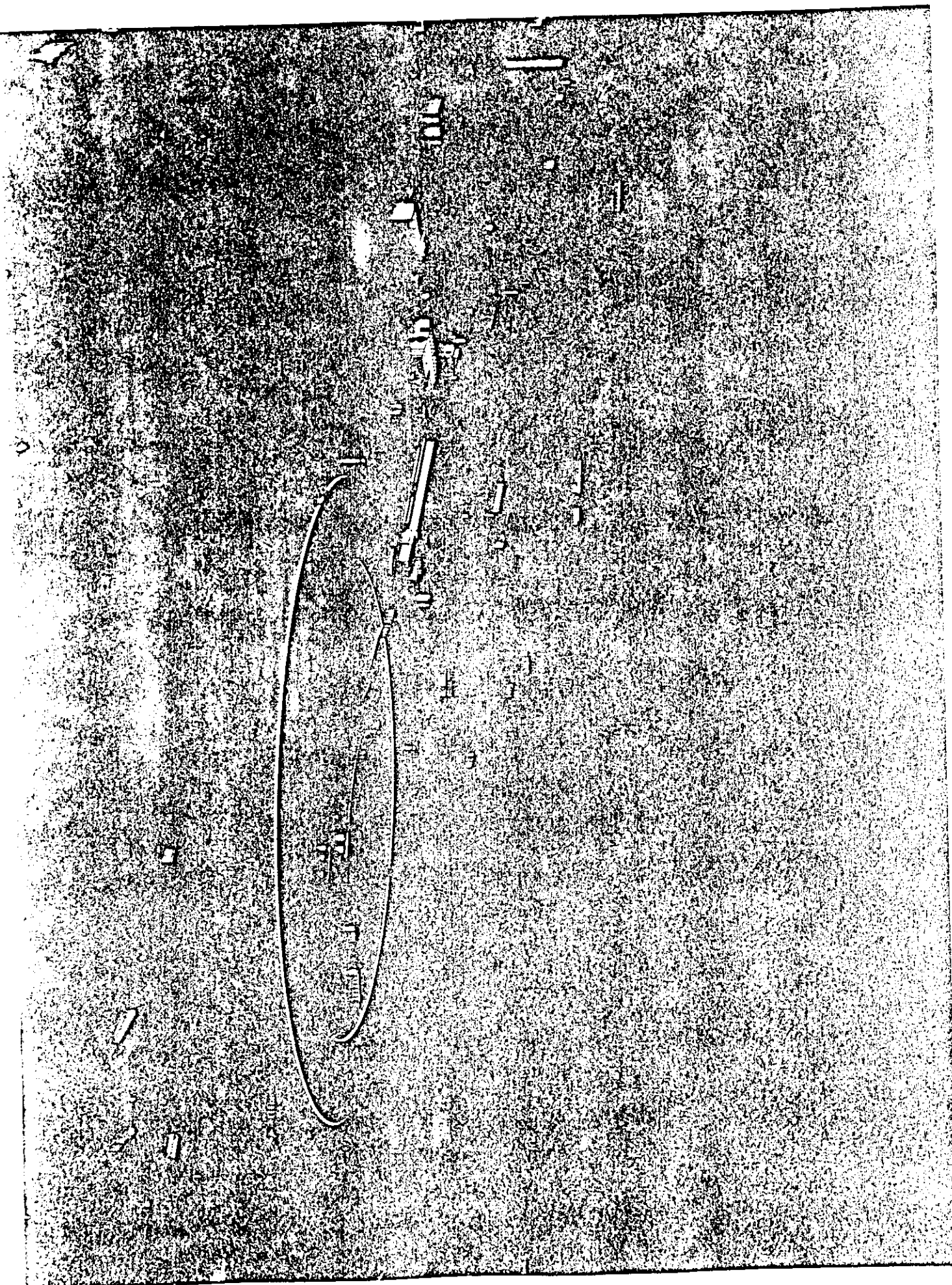
$$n\lambda = \frac{\lambda_0}{2\gamma^2} \left( 1 + \frac{K^2}{2} \right)$$

$$n = 1, 3, 5, \dots$$

Off-axis

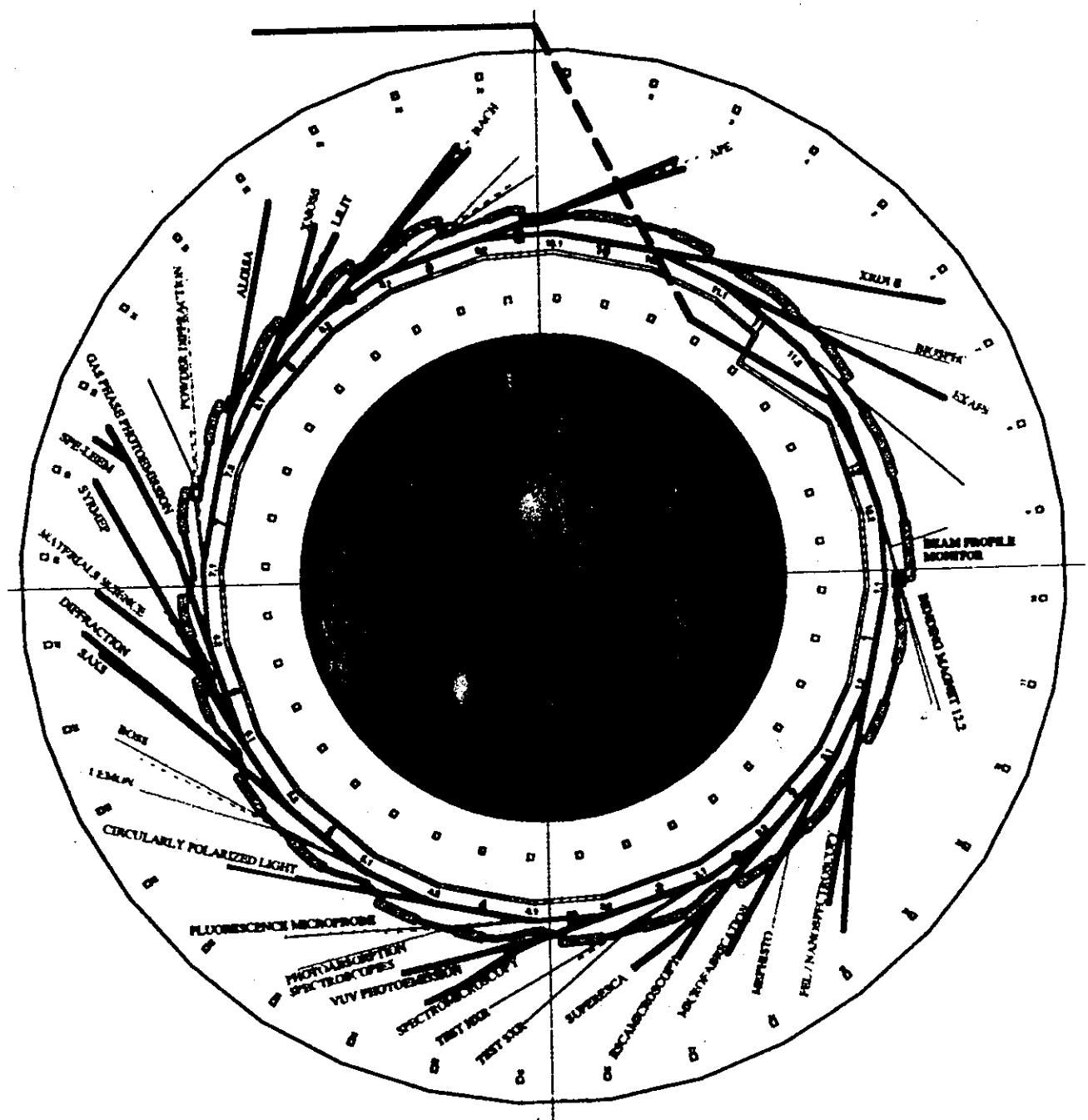
$$n\lambda = \frac{\lambda_0}{2\gamma^2} \left( 1 + \frac{K^2}{2} + \gamma^2 \theta^2 \right)$$

$$n = 1, 2, 3, \dots$$





# ELETTRA LAYOUT



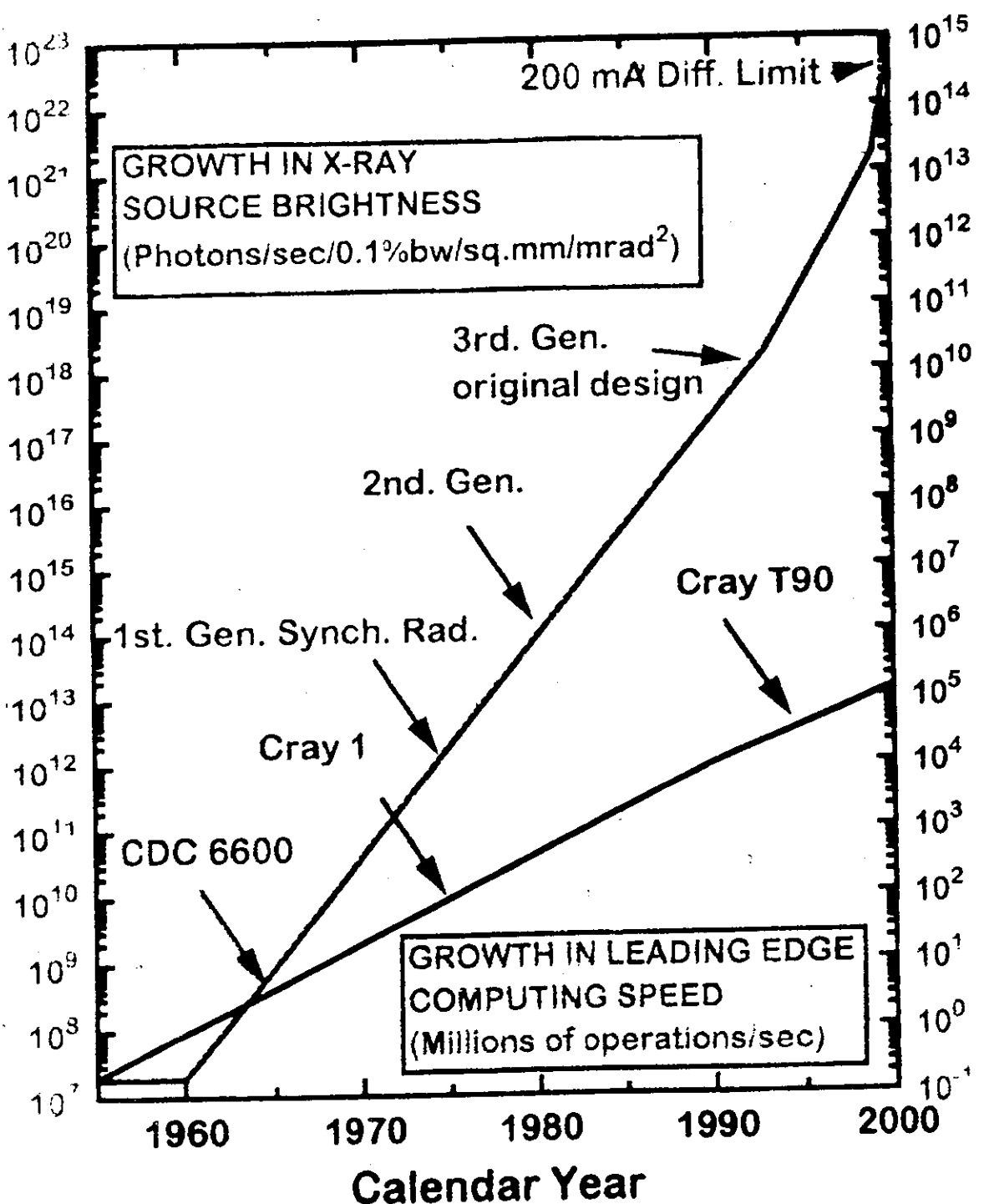
AS: 10/12/98

## **BRILLIANCE / SPECTRAL BRIGHTNESS**

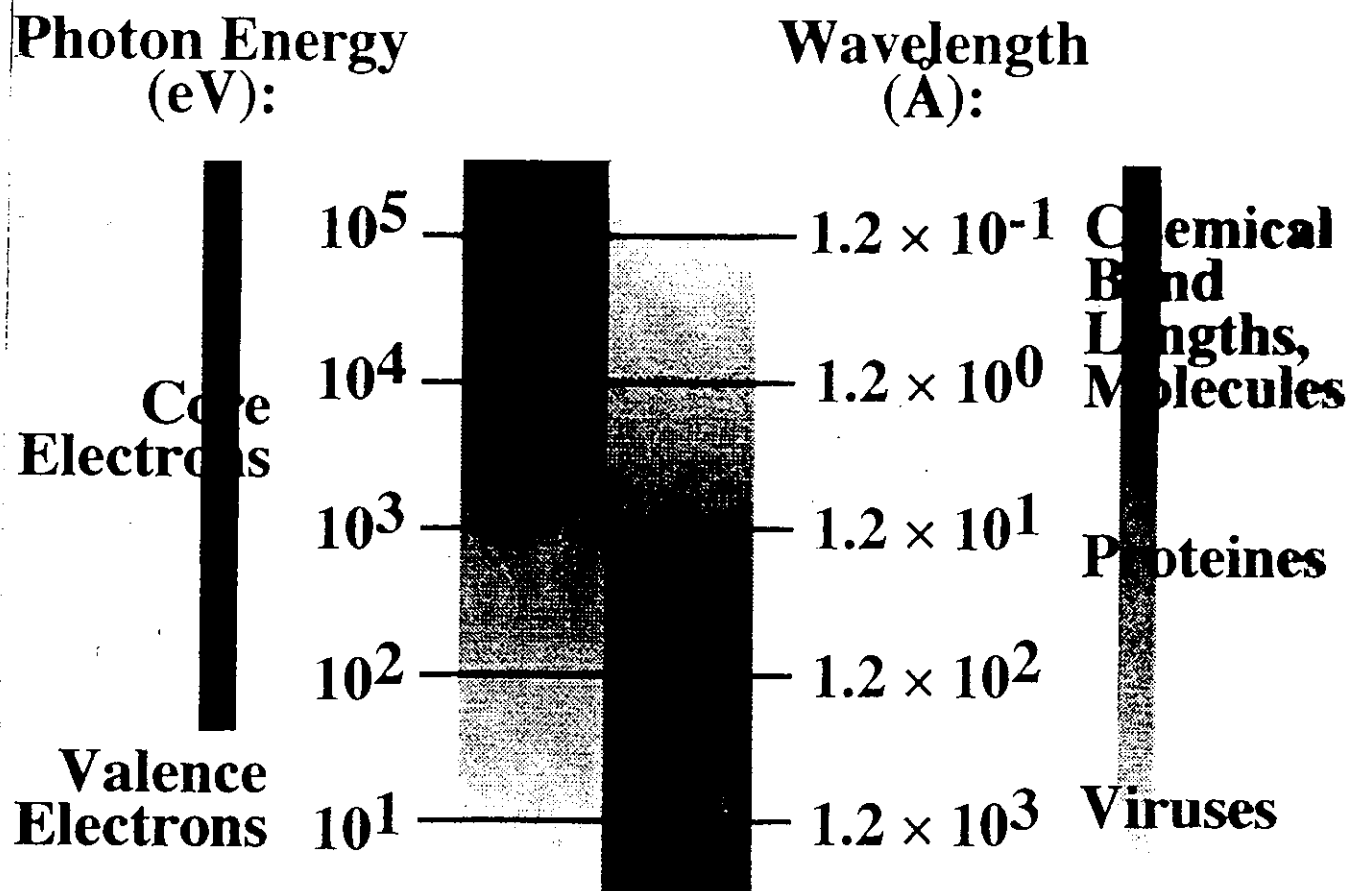
**FLUX OF PHOTONS IN UNIT WAVELENGTH RANGE**  
-----  
**(SOURCE AREA) (BEAM DIVERGENCE)**

**UNITS:**

**Photons/s/mm<sup>2</sup>/mrad<sup>2</sup>/0.1% bandwidth**



# **IMPORTANCE OF SYNCHROTRON LIGHT:**



# Photoemission

# Spectroscopy

A fundamental probe  
of the electronic  
structure of

- solids
- solid surfaces
- adsorbates

# Photoemission      Spectroscopy

U P S - Ultraviolet

From valence electrons.

X P S - X-ray

From core levels

A R U P S - Angle-resolved  
(A R P E S)                  Ultraviolet

Momentum - dependence of electron  
excitations, especially in quasi  
2-dim.    systems

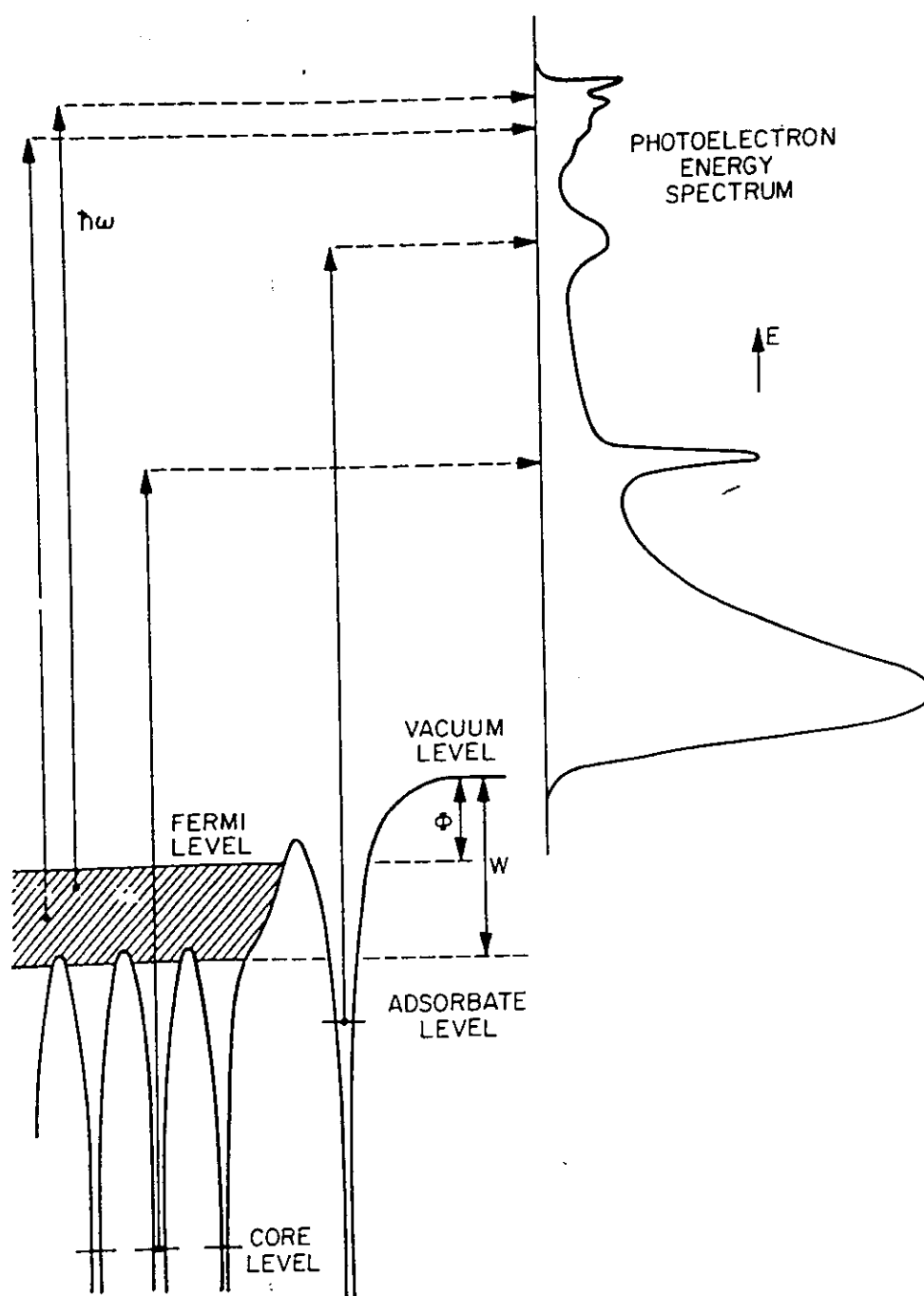
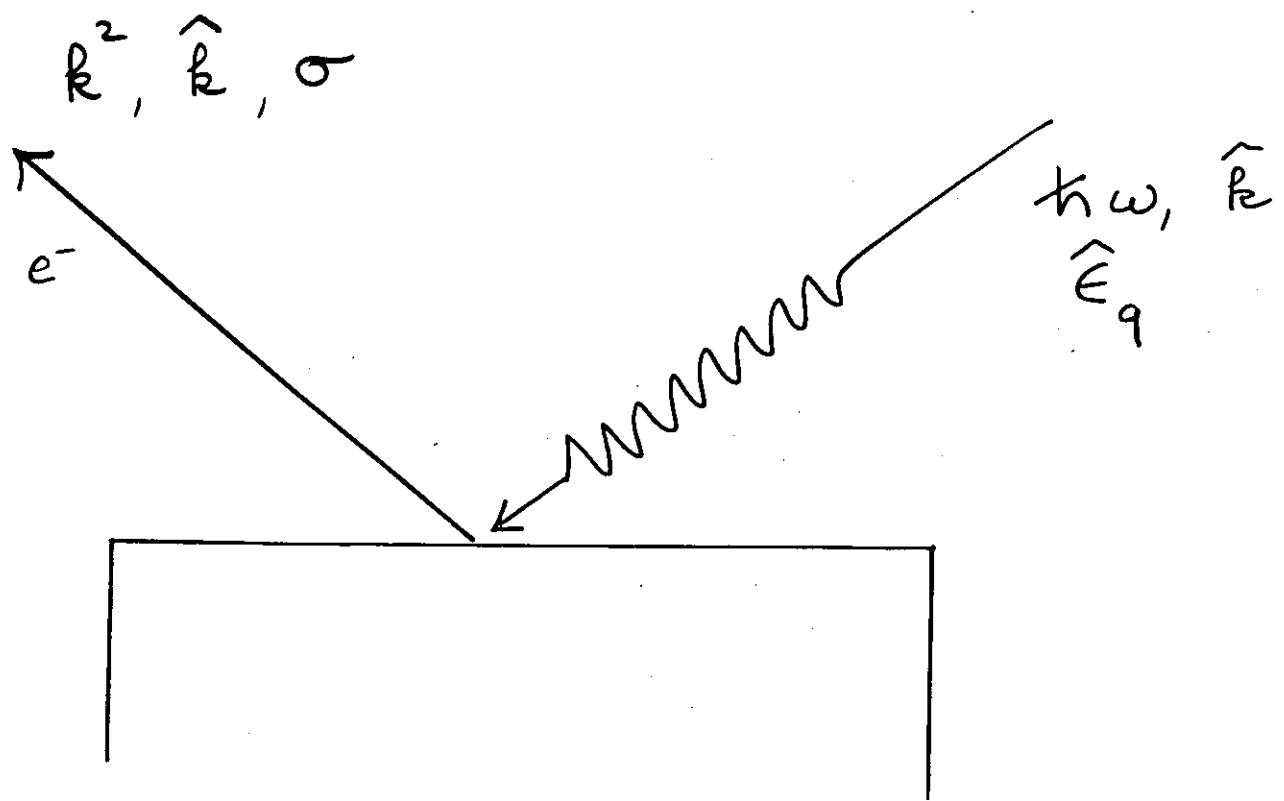


Fig. 1. Energetics of photoemission from a metallic solid, showing schematically the electronic potential, core levels, an adsorbate level, valence band (cross-hatched) and typical photoelectron energy spectrum at photon energy  $\hbar\omega$ . The work function  $\Phi$  and the inner potential  $W$  are indicated.

levels, and this applies to the study of atoms and molecules as well as solid surfaces.

Other processes can contribute to the measured spectrum. The refilling of core holes can provide enough energy to eject extra electrons (Auger electrons) which are characterized by a  $\hbar\omega$ -independent kinetic energy. In the case of solids, photoelectrons which have undergone an inelastic scattering can still be



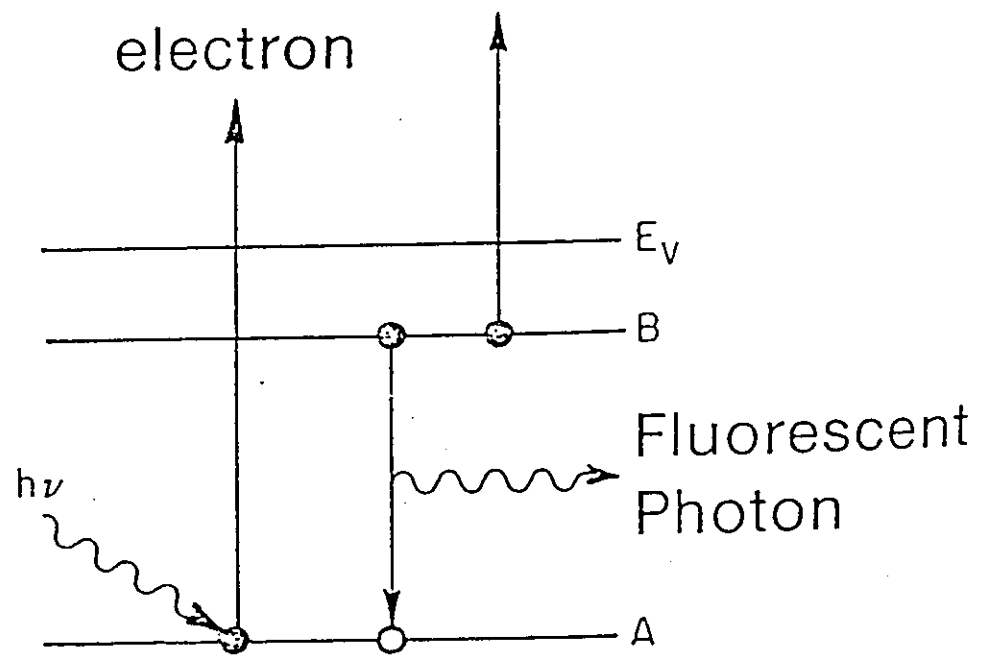
Electron :

- Energy
- Direction (angle)
- Spin

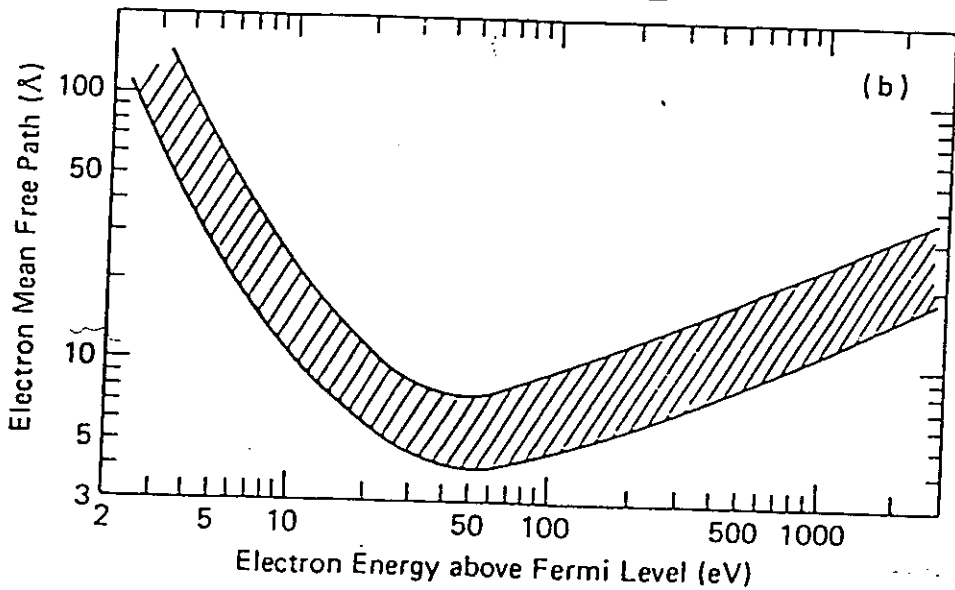
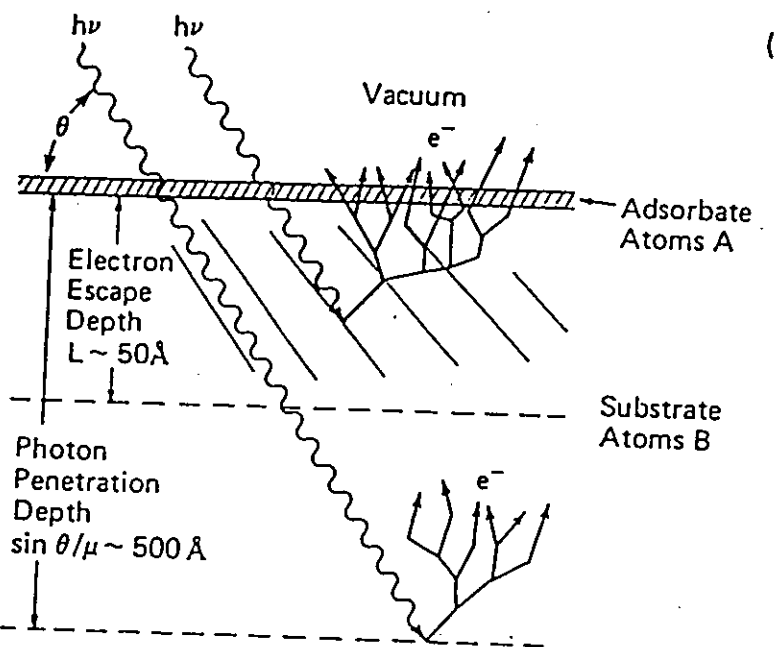
Photon

- Energy
- Polarization
- [ - Direction ]

Auger  
Photo- Electron  
electron



(5.1)



5.6

ADS44B

# One-electron theory of Photoemission:

$$\sigma \sim \sum_{i,f} p_i | \langle \psi_i(\vec{r}) | \vec{A} \cdot \vec{p} | e^{i\vec{k}_f \cdot \vec{r}} \rangle |^2$$

$$\delta(E_i + \hbar\omega - \frac{\hbar^2 k_f^2}{2m}) \delta(\frac{\hbar k_f^2}{2m} - E_f)$$

Constant M.E. approximation:

$$\sim \sum_{i,f} p_i \delta(E_i + \hbar\omega - E_f)$$

$$= \rho(E_i - (E_f - \hbar\omega))$$

"Displaced density of states"

Many-body generalized  
formulation.

$$g(E) \iff -\frac{1}{\pi} \operatorname{Im} G(E)$$

In ARUPS experiments, where  
 $\hat{k}_f$  is also detected,

$$\begin{aligned}\sigma &\sim -\frac{1}{\pi} \operatorname{Im} G(\vec{k}, E) \\ &= A(\vec{k}, E)\end{aligned}$$

Electron  
function

Number of electrons that can be  
removed weighted by the rearrange-  
ment of all others.

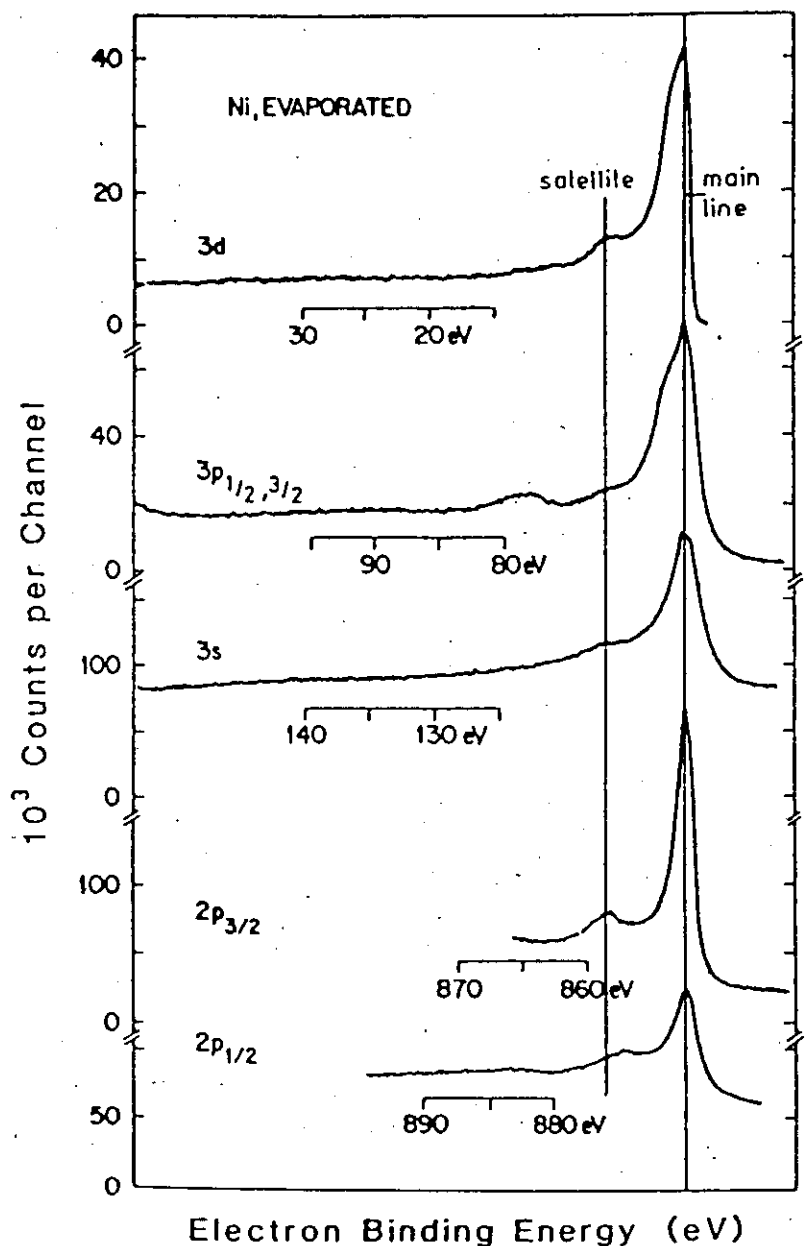


Fig.3.13. XPS spectra of the 3d, 3p, 3s, 2p<sub>3/2</sub> and 2p<sub>1/2</sub> levels of Ni metal [3.10]. The main lines have been lined up to demonstrate the constant distance of the satellite position (even for the 3d valence band)

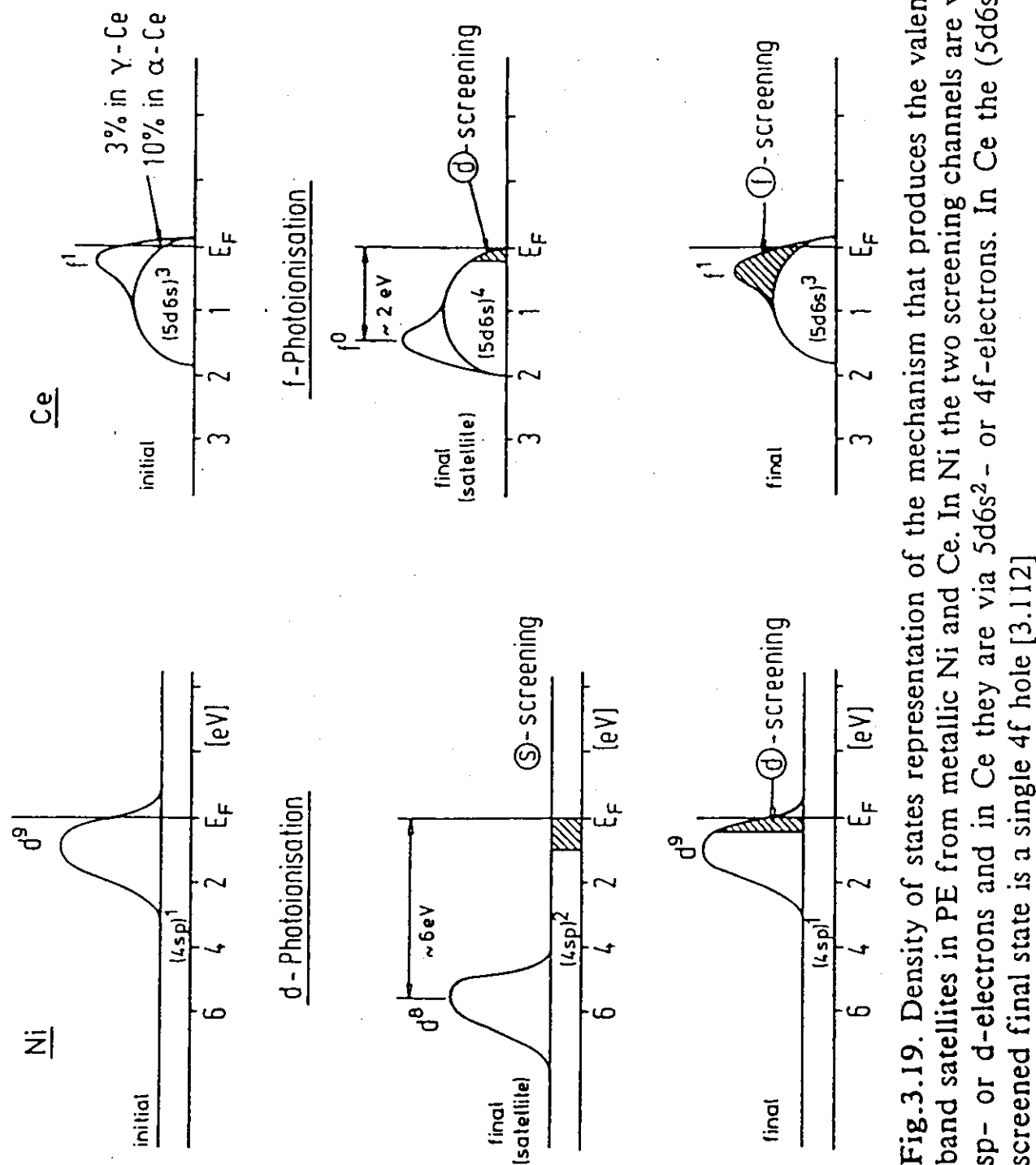


Fig.3.19. Density of states representation of the mechanism that produces the valence band satellites in PE from metallic Ni and Ce. In Ni the two screening channels are via sp- or d-electrons and in Ce they are via  $5d6s^2$ - or 4f-electrons. In Ce the  $(5d6s)^4$  screened final state is a single 4f hole [3.112]

## Many - body effects

Ground state of metallic

Ni :

$$\langle n_d \rangle \sim 9.2 - 9.4$$

Mixing of atomic configurations:

$$\alpha (3d^9 4s) + \beta 3d^{10} + \gamma (3d^8 4s^2)$$

$\gamma^2 \ll 1$

Photoemission final states:

$$(3d^8 4s, \vec{k}_f) \quad \text{and} \quad (3d^9, \vec{k}_f)$$

### Ni-metal, core photoionization

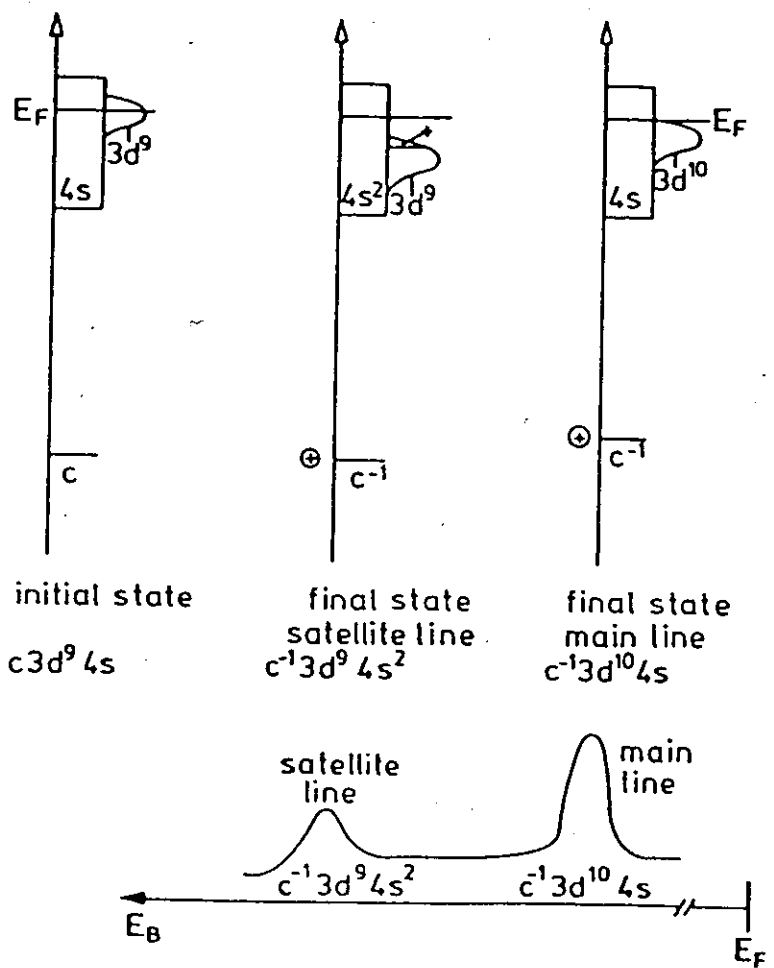
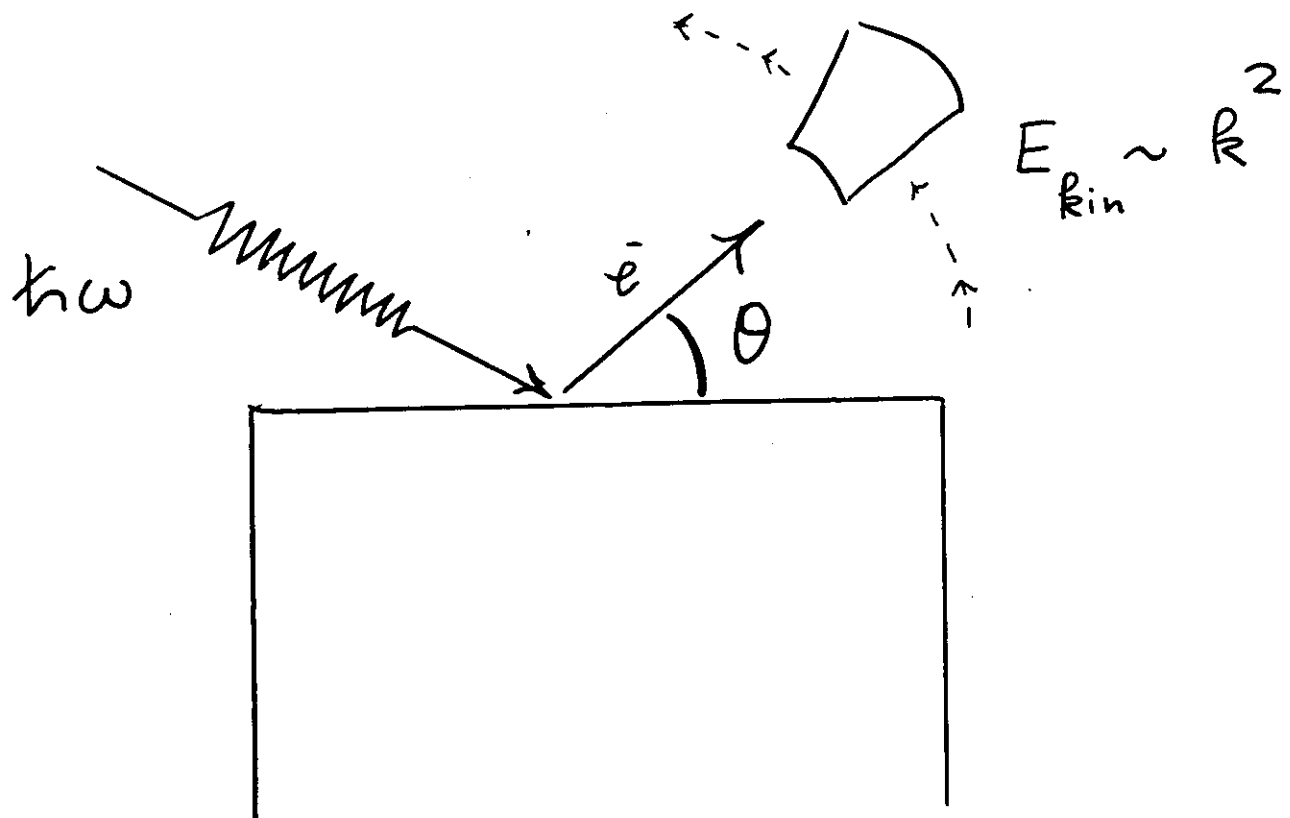


Fig.3.14. Schematic density of states of Ni, indicating the origin of the main line and the satellite for core ionization ( $c^{-1}$ ); for valence band ionization see also Fig.3.19. The initial state is  $c3d^94s$  and the two final states are  $c^{-1}3d^94s^2$  (satellite) and  $c^{-1}3d^{10}4s$  (main line);  $c$  denotes a core level,  $c^{-1}$  a core hole



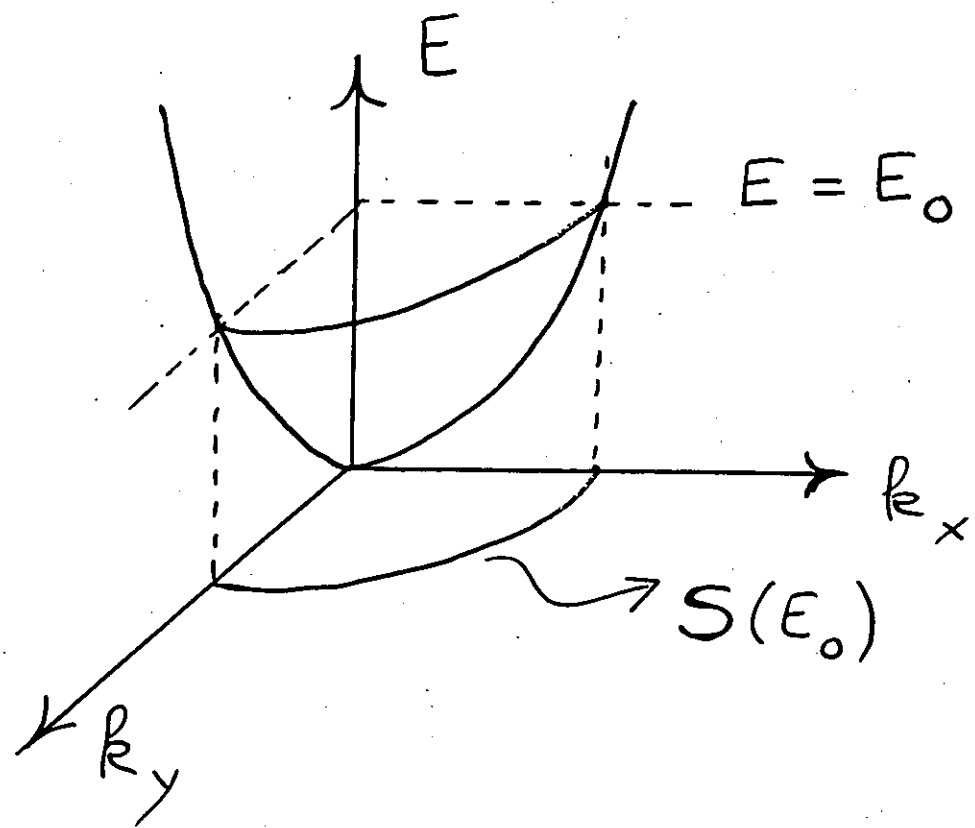
$$E_{\text{kin}} \sim R^2 = R_{\parallel}^2 + R_{\perp}^2$$

$$k_{\parallel} / \text{\AA}^{-1} = 0.51 \sin \theta \sqrt{E_{\text{kin}} / \text{eV}}$$

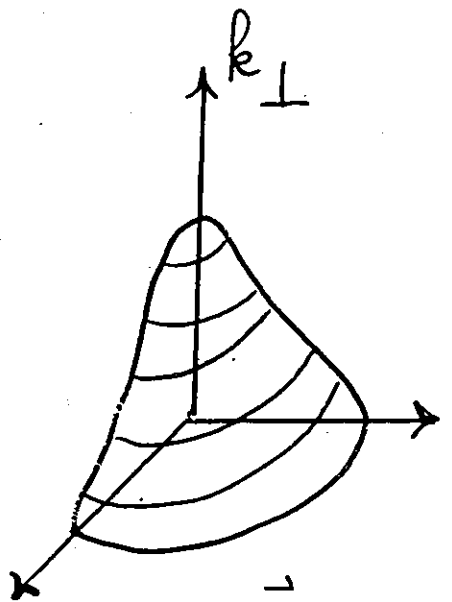
In the photoemission process,  $\vec{k}_{\parallel}$  is conserved, but  $\vec{k}_{\perp}$  is not!

(Breaking of  $\perp$  translation symmetry by the sample termination at the surface.)

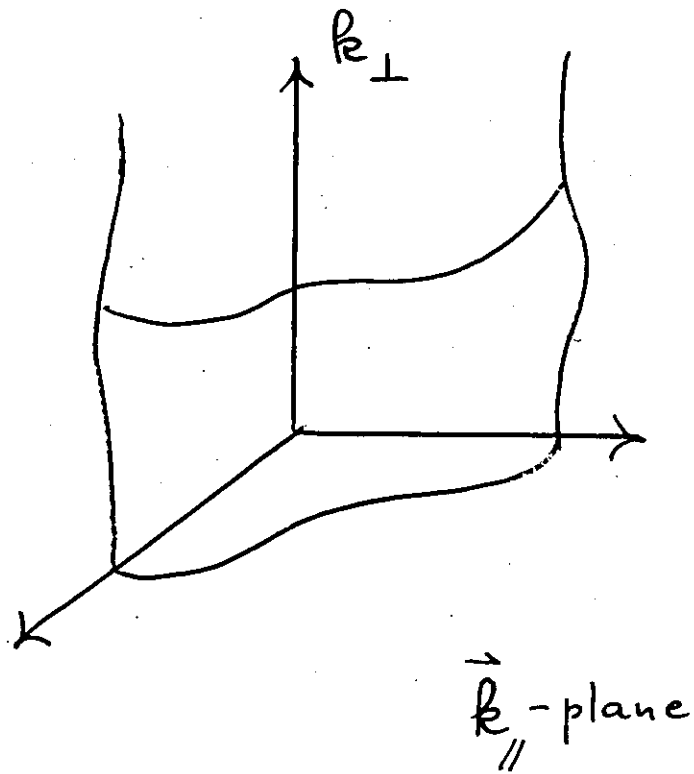
Band structure and constant energy surfaces.



3-dim. solid



Quasi 2-dim. solid



Example of quasi 2-dim.  
solids:

the High-Temperature Cuprate  
Superconductors

Ding et al.

Phys. Rev. Lett. 76, 1533 (96)

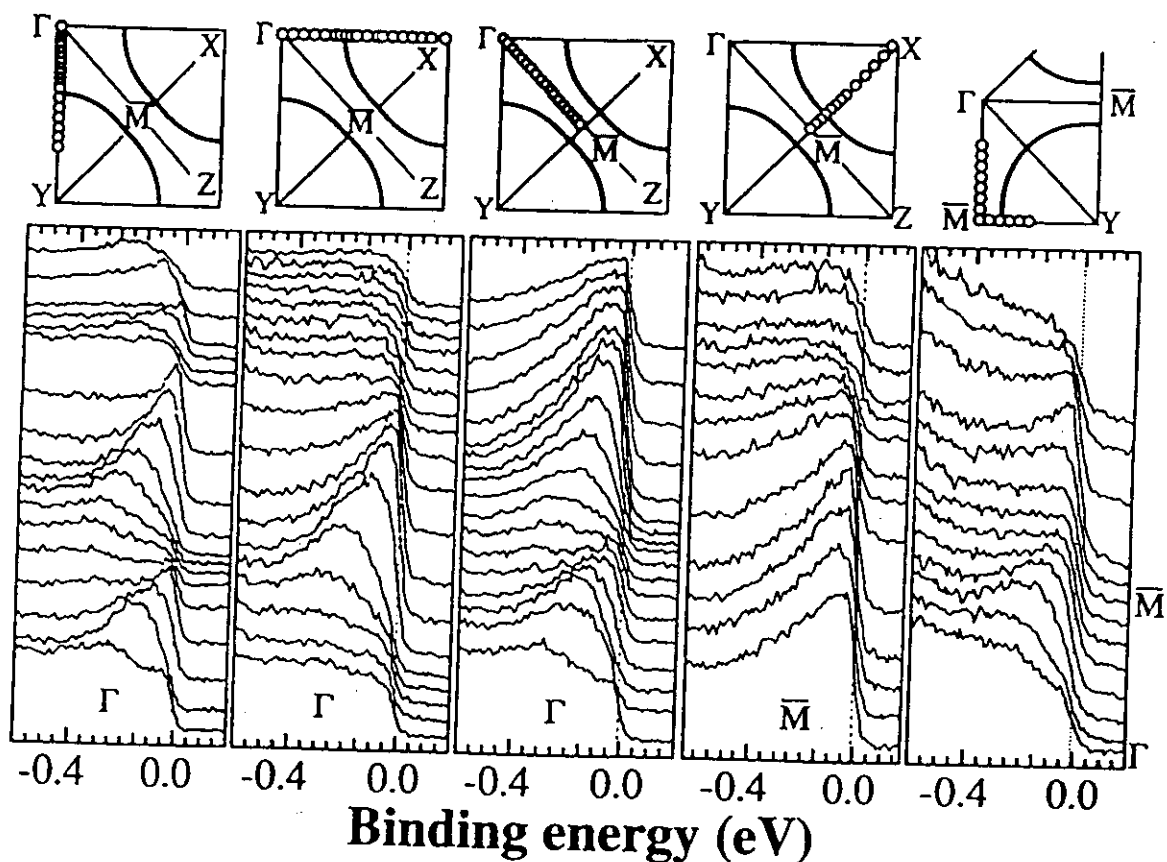


FIG. 1. Normal state ( $T = 95$  K) EDC's of Bi2212 along various symmetry lines at values of the momenta shown as open circles in the upper insets. The photon polarization  $\mathbf{A}$  is horizontal in each panel.



Marshall et al.  
Phys. Rev. Lett. 76,

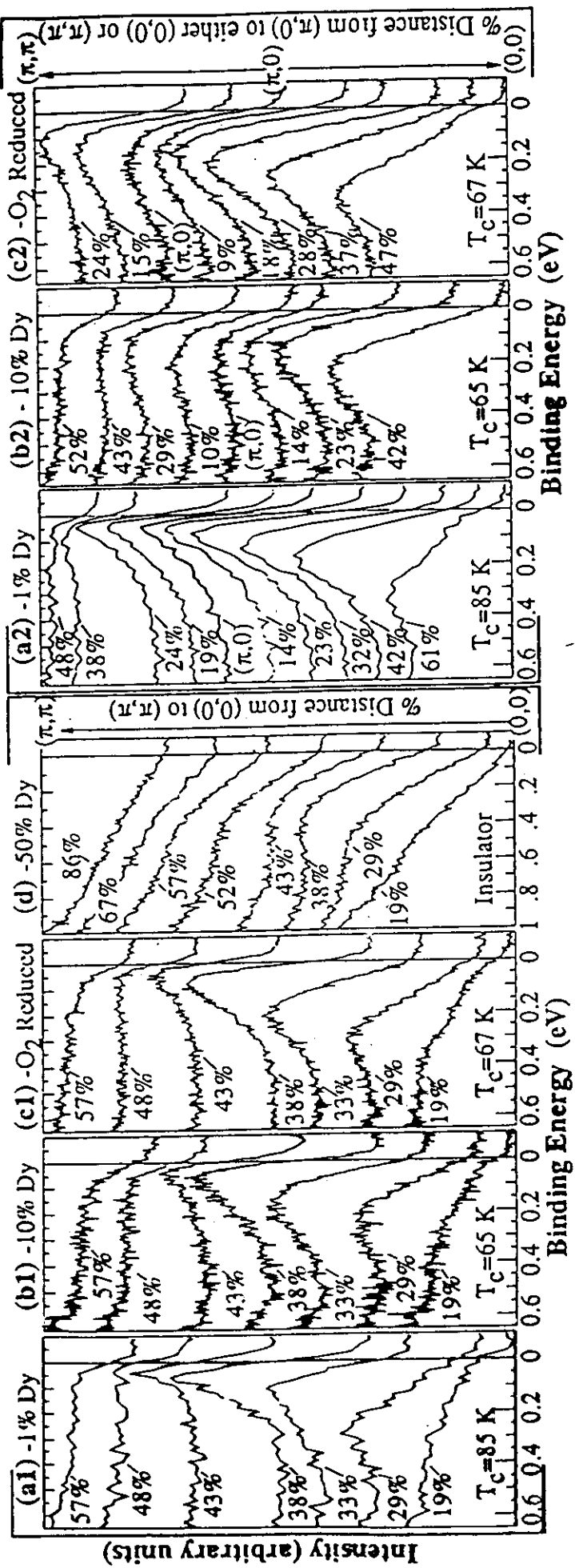


FIG. 1. ARPES spectra from  $\text{Bi}_2\text{Sr}_2\text{Ca}_{1-x}2\text{Dy}_x\text{Cu}_2\text{O}_{8+\delta}$  single crystal thin films and deoxygenated  $\text{Bi}_2\text{Sr}_2\text{Ca}\text{Cu}_2\text{O}_{8+\delta}$  crystals. The symmetry points identified correspond to those indicated in the two-dimensional Brillouin zone of Fig. 4.

Marshall et al.

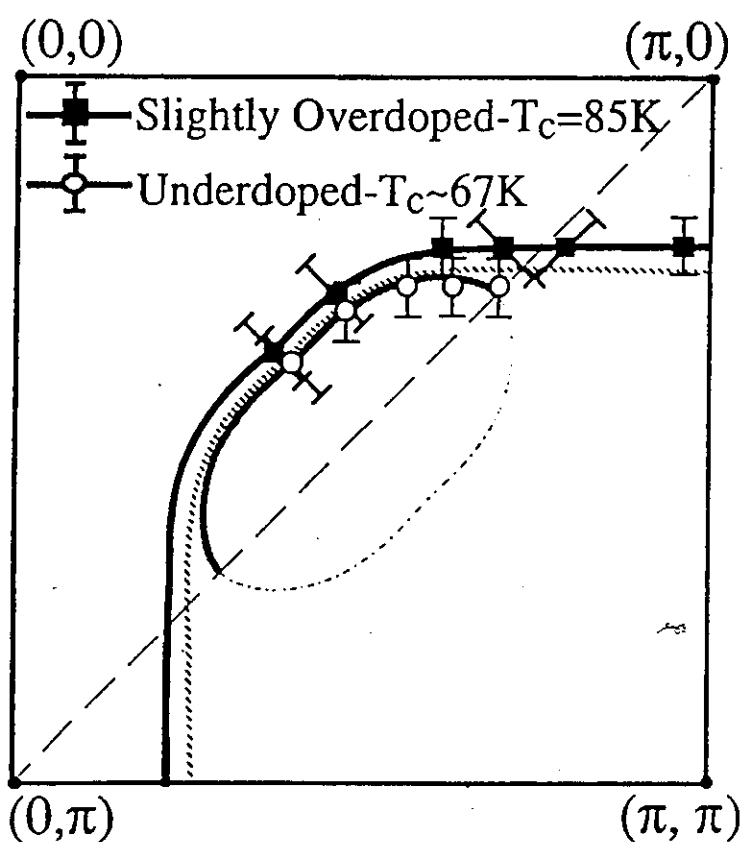
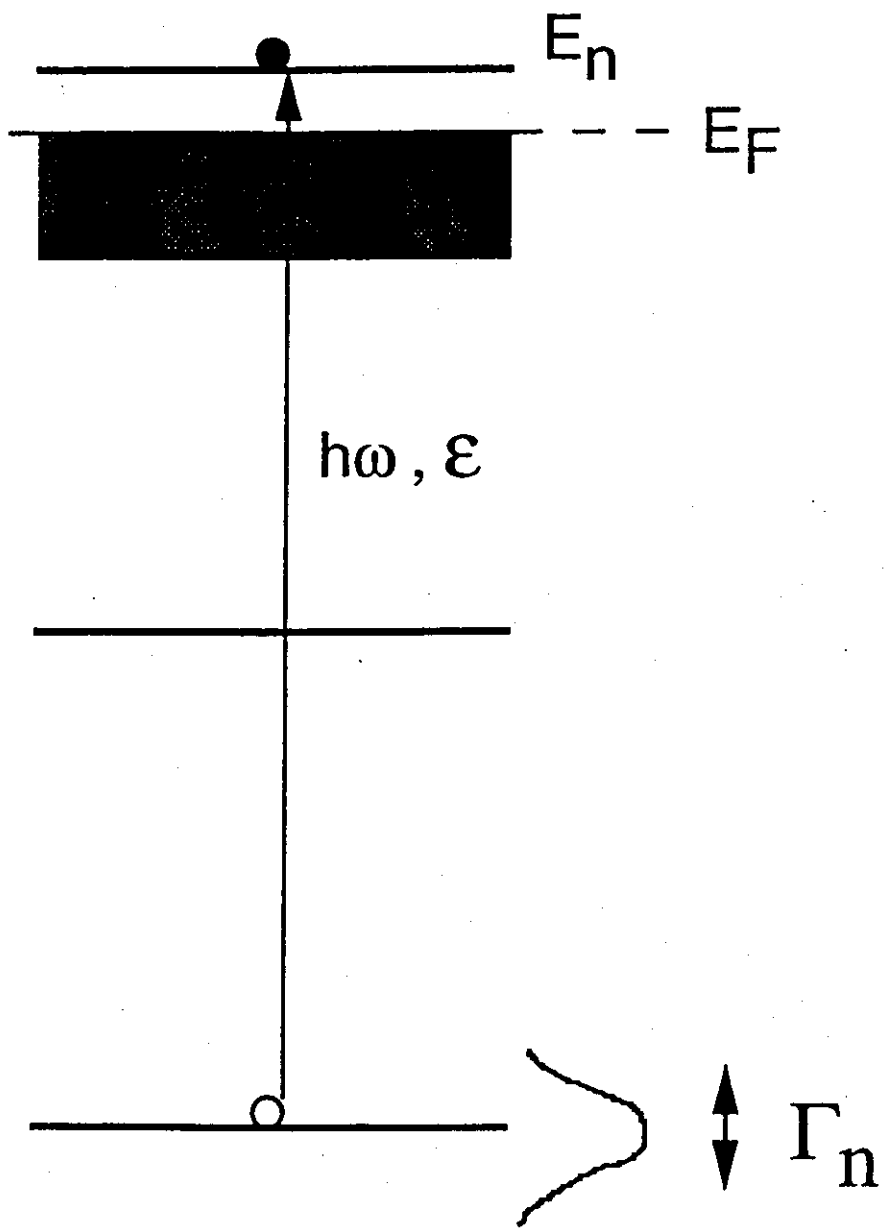
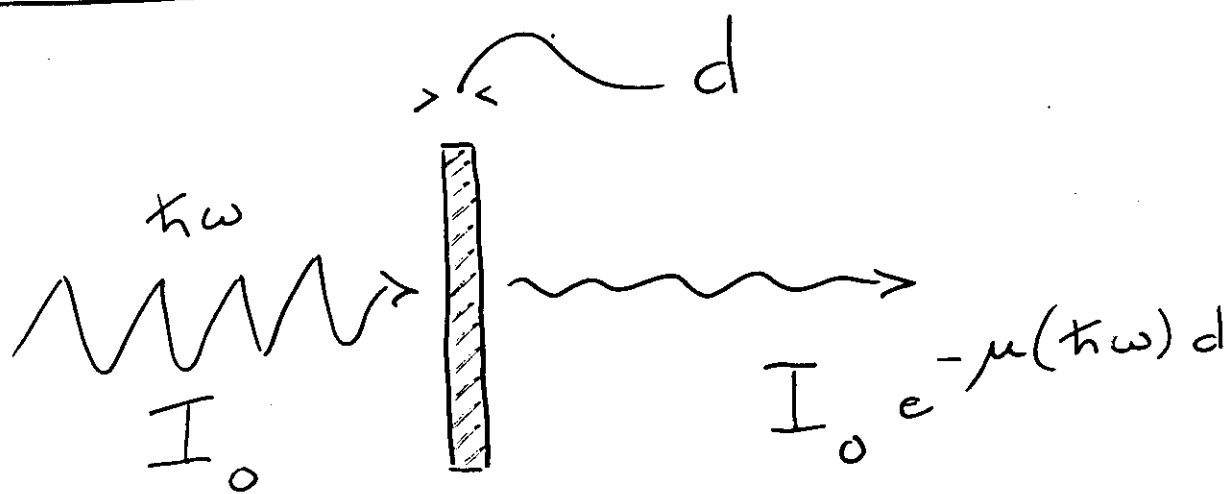


FIG. 4. Fermi level crossings from two Bi2212 samples of differing oxygen content. The entire BZ can be reconstructed by fourfold rotation about  $(0,0)$ .



## Dichroism

①



►  $\mu(\hbar\omega)$  = Absorption coefficient

► Relationship with microscopic quantities:

$N$  = # of atoms / unit volume

$\sigma_{at}$  = atomic absorption cross section =

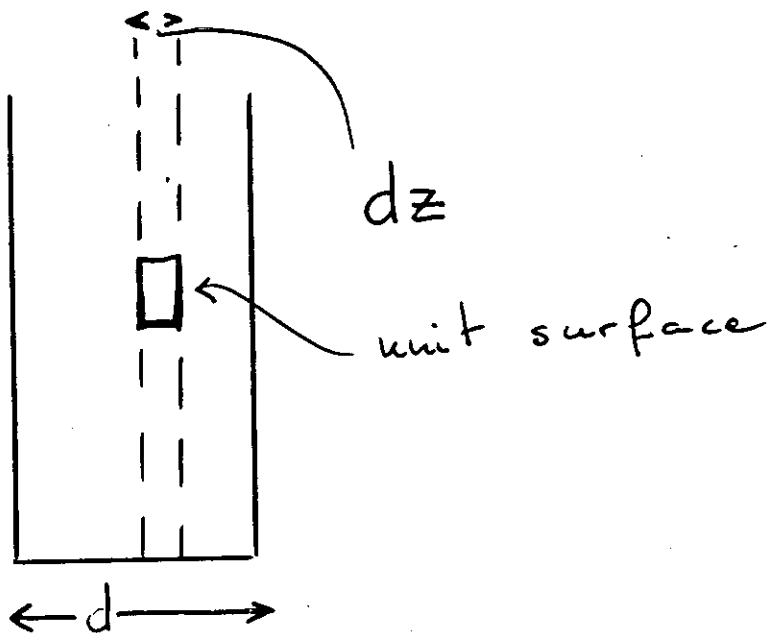
$$= \frac{\text{# of photons absorbed by atom in unit time}}{\text{# photons incident per unit surface per unit time}}$$

$$\rightarrow N = I_0 / \hbar\omega$$

$$\mu(\hbar\omega) = N \cdot \sigma_{at}$$

(2)

## Dichroism



Photons absorbed between  $z$  and  $z + dz$ :

$$dN^P(z) = -N(z) \cdot \sigma_{at} \cdot N dz$$

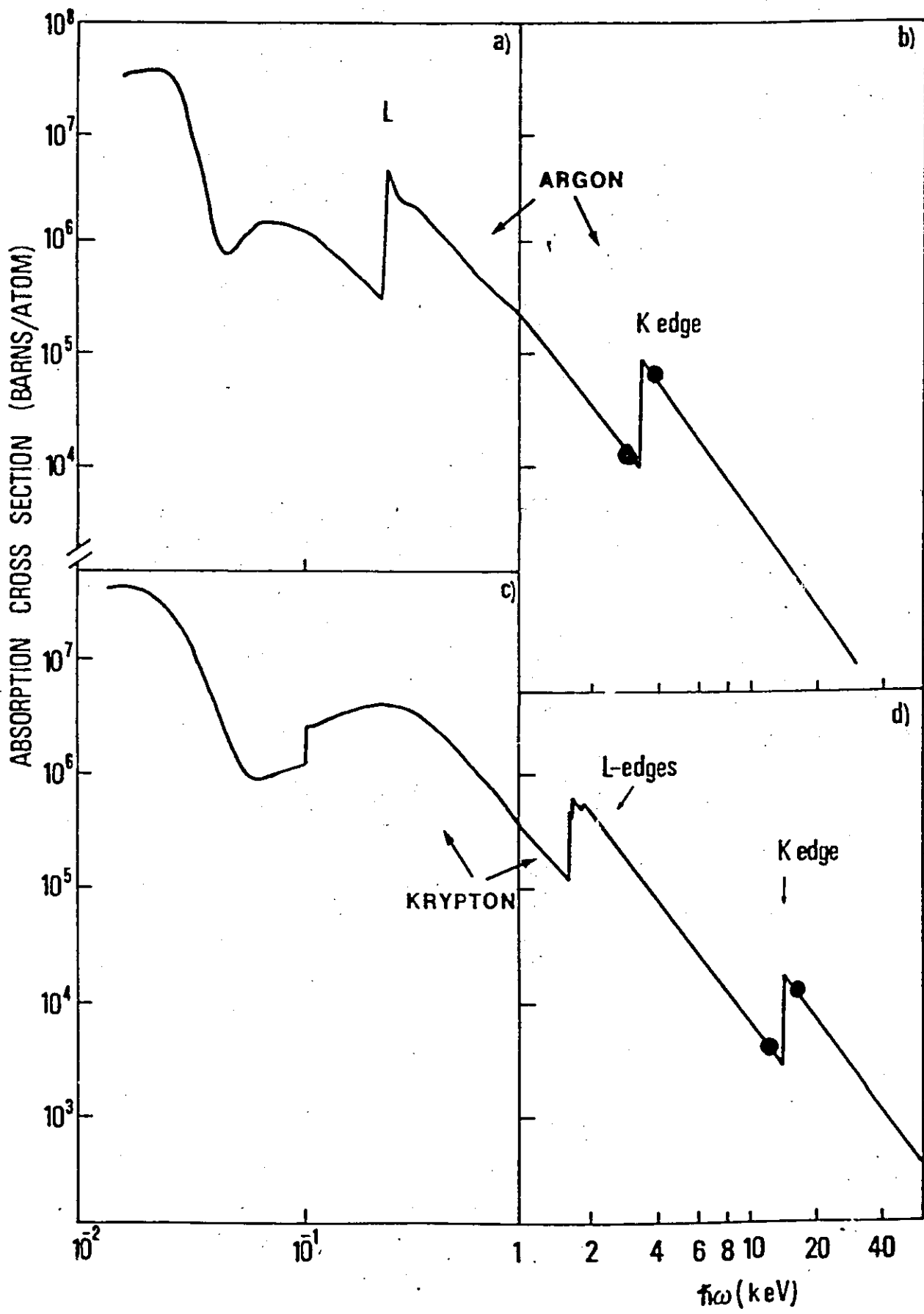
$$\left\{ \begin{array}{l} \frac{dN^P(z)}{dz} = -N \sigma_{at} \quad N^P(z) \\ N(0) = N_0 \end{array} \right.$$

$$\rightarrow N^P(z) = N_0 e^{-N \sigma_{at} \cdot z}$$

$$\rightarrow \mu = N \sigma_{at} \quad \text{QED}$$

### 11.3. ATOMIC ABSORPTION

583



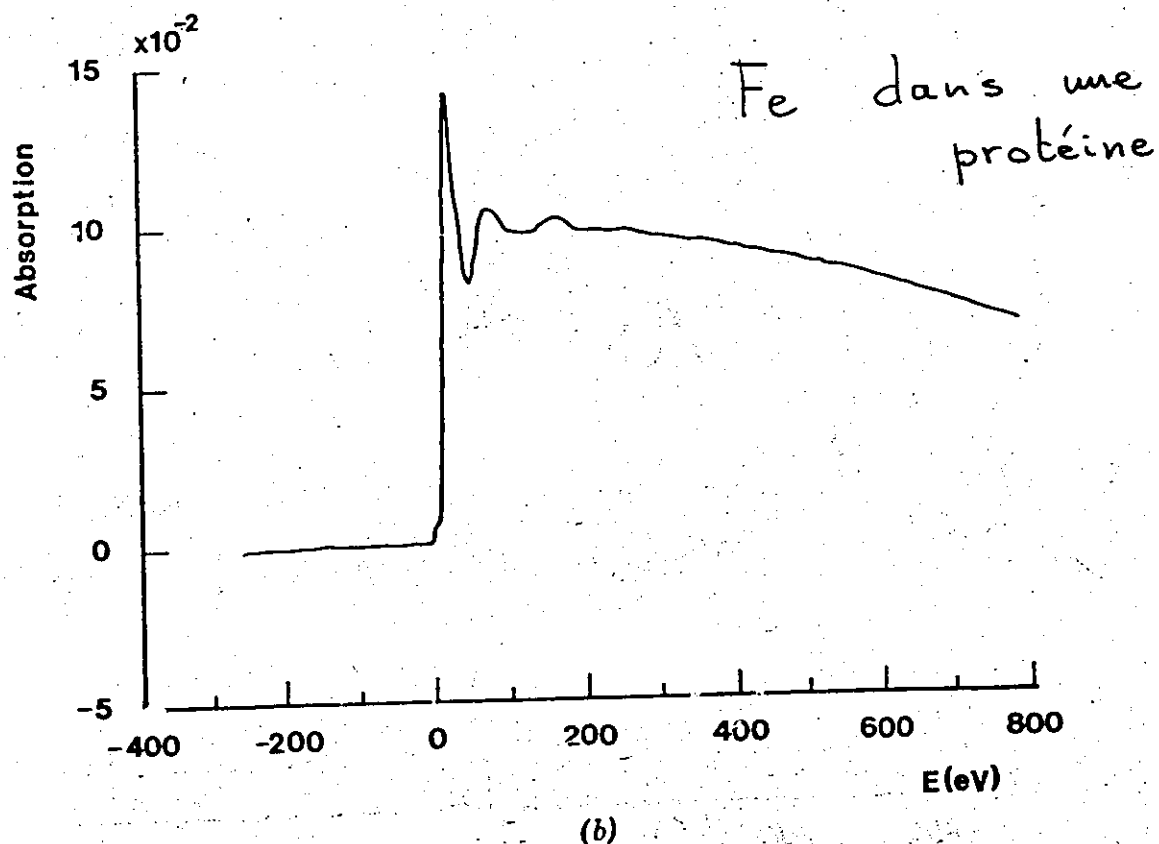
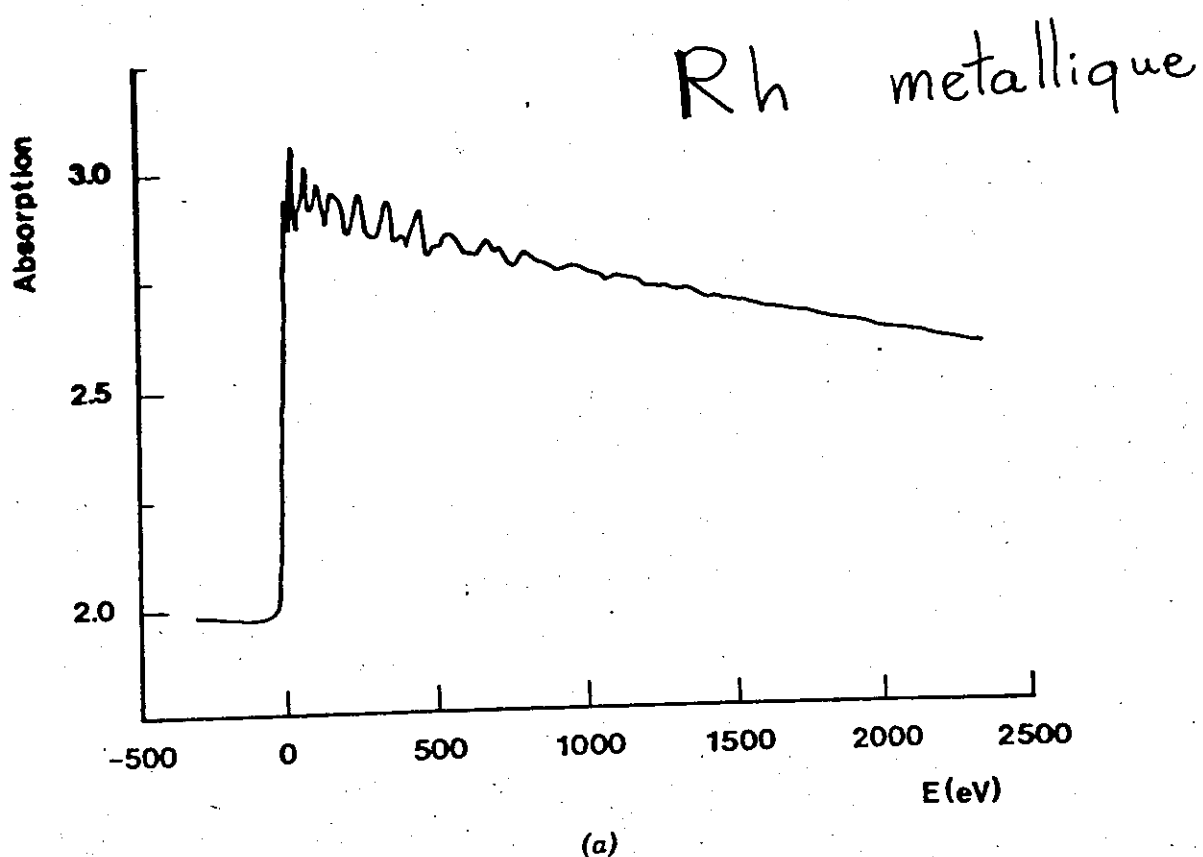


Figure 6.1: Raw absorption versus photoelectron energy for (a) the rhodium K-edge (23220 eV) in rhodium metal foil at 80 K and (b) the iron K-edge (7112 eV) in the protein ferritin taken in the fluorescence model. (c) The normalized absorption spectrum for the rhodium foil data in (a). A Victoreen pre-edge function has been used and the spectrum normalized at 107 eV above the edge. (d) The normalized fluorescence spectrum for the ferritin data of (b). A linear pre-edge function was removed and the spectrum normalized at 95 eV above the edge.

## DATA ANALYSIS

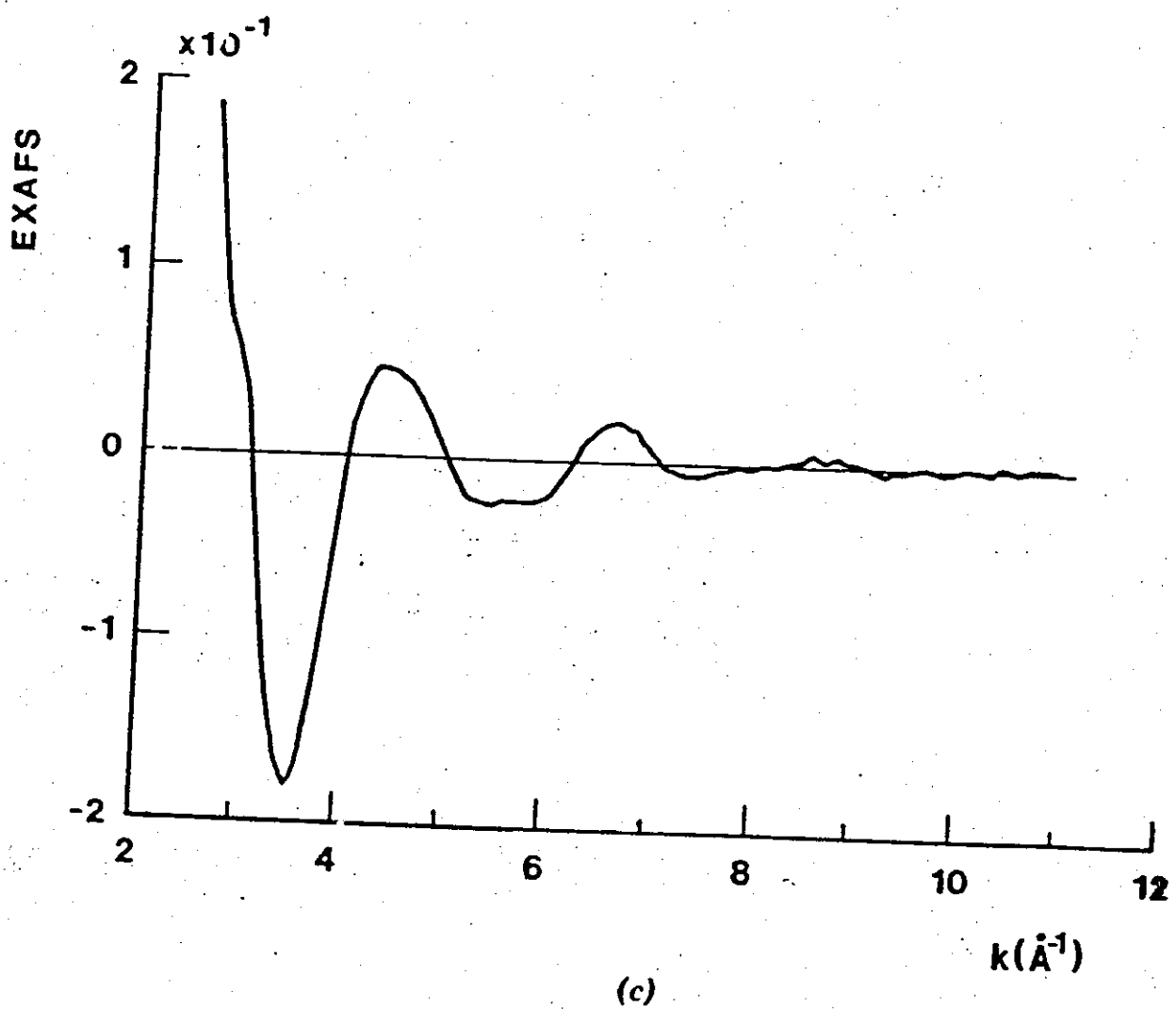


Figure 6.3. (Continued)

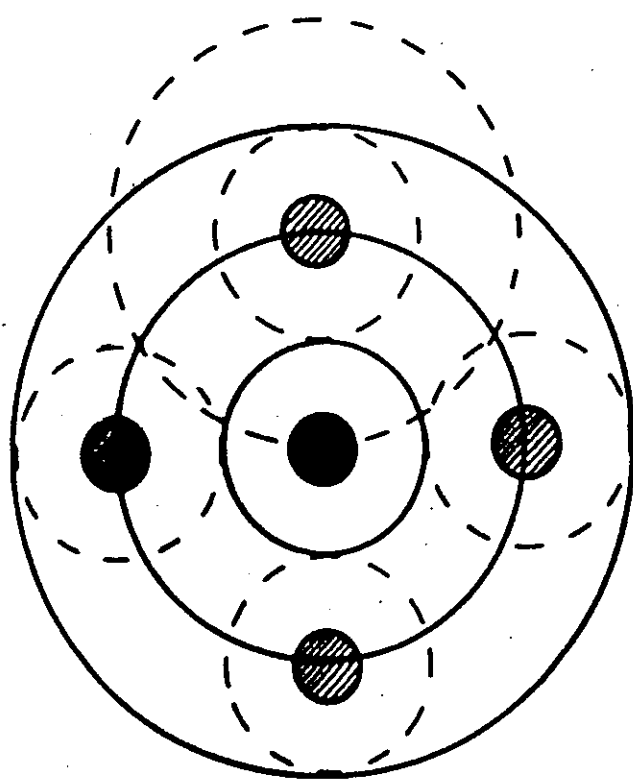
$$\chi(k) = \sum_j N_j S_0^2(k) F_j(k) \exp(-2k^2 \sigma_j^2)$$

# EXAFS

Extended X-ray Absorption  
Fine Structure

Local structural probe

Atomic arrangement around specific  
atom, selected by choice of  
abs. threshold.



# X-Ray Absorption & Photoemission

- \* Absorption threshold (XANES) (mostly electronic)
- \* EXAFS (extended absorption fine structure: mostly structural)

Absorption from core levels:  
validity of the multipole expansion.

$$\sigma_{\text{abs}}(\omega) \sim \sum_{i,f} |\langle \psi_i | T | \psi_f \rangle|^2 \delta(E_i + \hbar\omega - E_f,$$

$$T = \vec{A} \cdot \vec{p} = A_0 e^{i \vec{k} \cdot \vec{r}} \vec{\epsilon} \cdot \vec{p}$$

$$\vec{\epsilon} = \text{polarization vector} \quad \vec{\epsilon} \cdot \vec{k} = 0 \Rightarrow [\vec{\epsilon} \cdot \vec{p}, e^{i \vec{k} \cdot \vec{r}}] = 0$$

$$\langle \psi_i | T | \psi_f \rangle \sim A_0 \int_{\text{core}} \psi_{i,\text{core}}(\vec{r}) e^{i \vec{k} \cdot \vec{r}} \vec{\epsilon} \cdot \vec{p} \psi_f(\vec{r}) d\vec{r}$$

$$|\psi_{i,\text{core}}(\vec{r})| \sim 0 \quad \text{for } |\vec{r}| \gg r_c$$

$$e^{i \vec{k} \cdot \vec{r}} \sim 1 + i \vec{k} \cdot \vec{r} + \dots$$

$$k r_c \ll 1$$

$$k r_c \ll 1$$

Relationship between core electron binding energy  $E_b$  and core radius  $r_c$ :

- $E_b \sim \frac{\hbar^2}{2m r_c^2}$

$$r_c \sim \hbar \sqrt{\frac{1}{2m E_b}}$$

- $k \equiv \frac{\omega}{c} \quad \omega \sim \frac{E_b}{\hbar}$

$$k = \frac{E_b}{\hbar c}$$

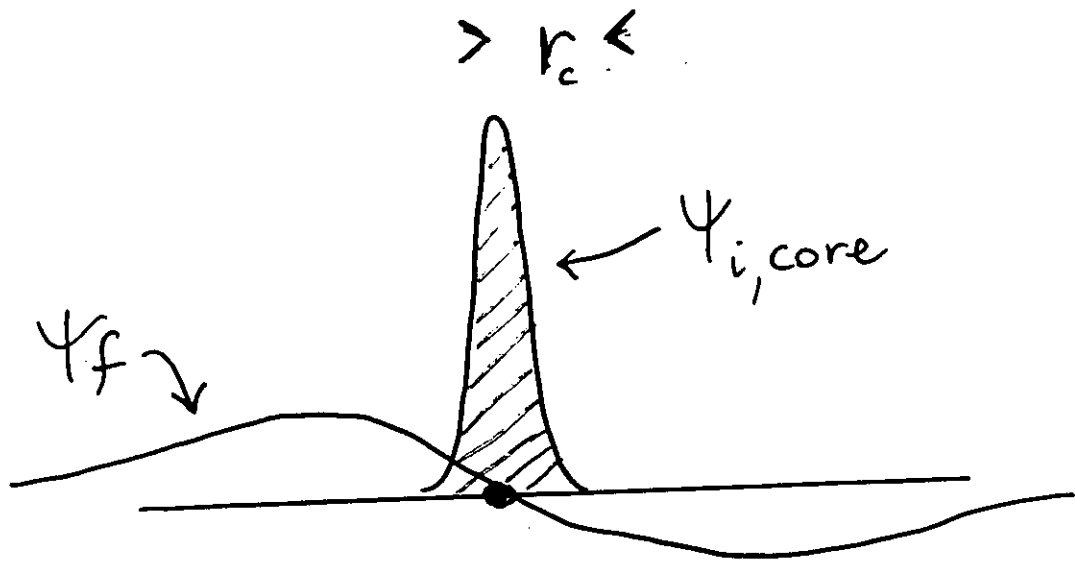
- $k r_c \sim \sqrt{\frac{E_b}{2mc^2}}$

$$2mc^2 \sim 1 \text{ MeV}$$

$$E_b \sim 0.115 \text{ MeV} \quad \text{for } 1s$$

electrons in U

$$\Rightarrow k r_c \ll 1$$



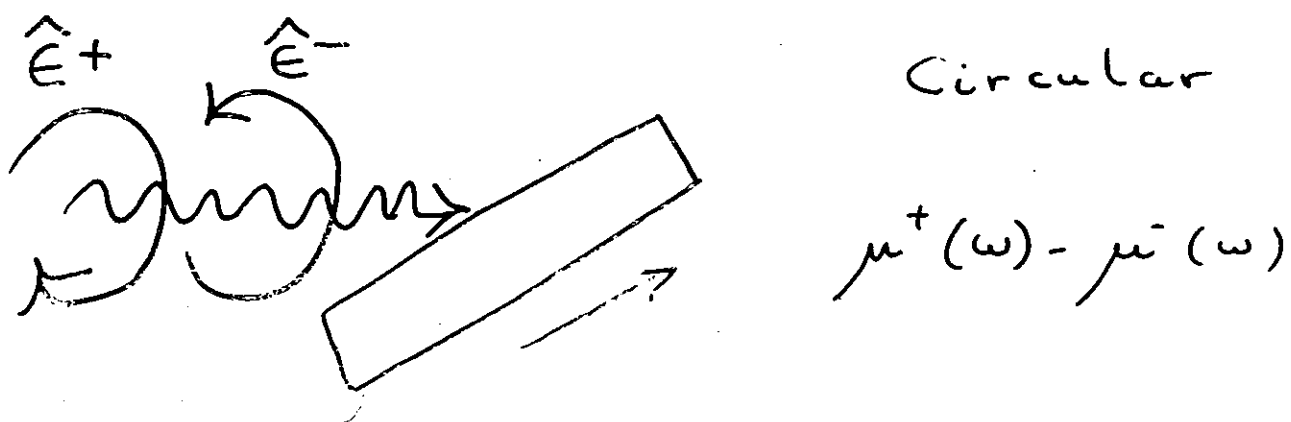
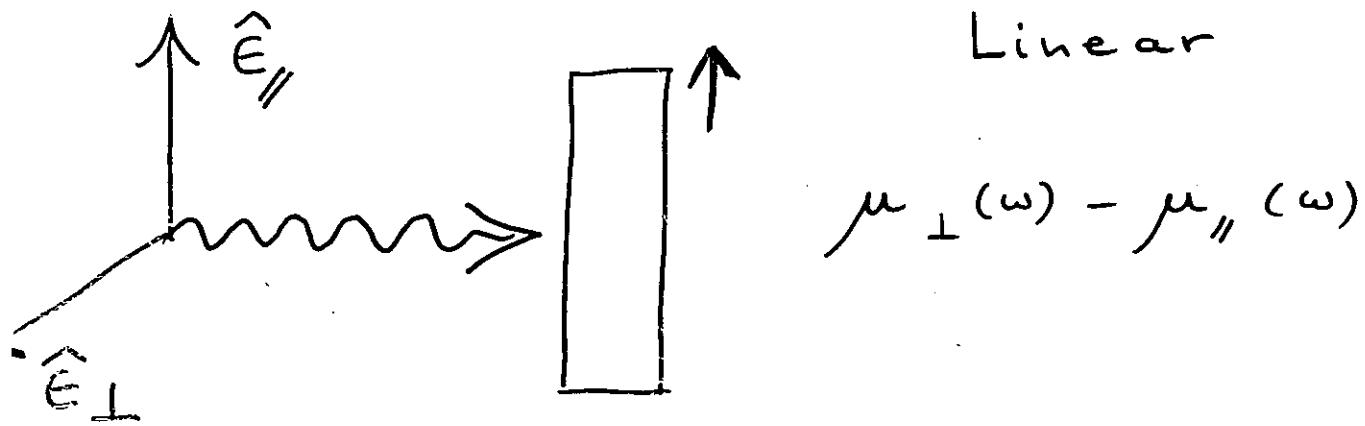
Matrix element

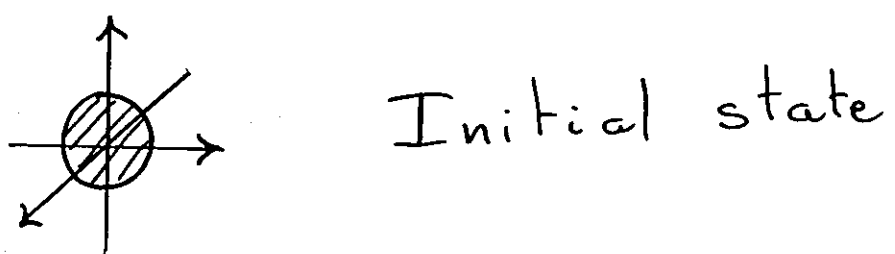
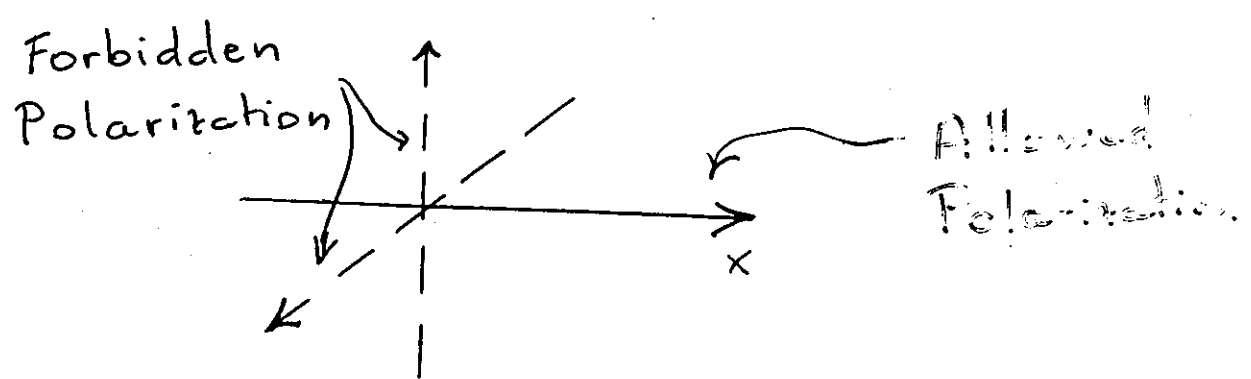
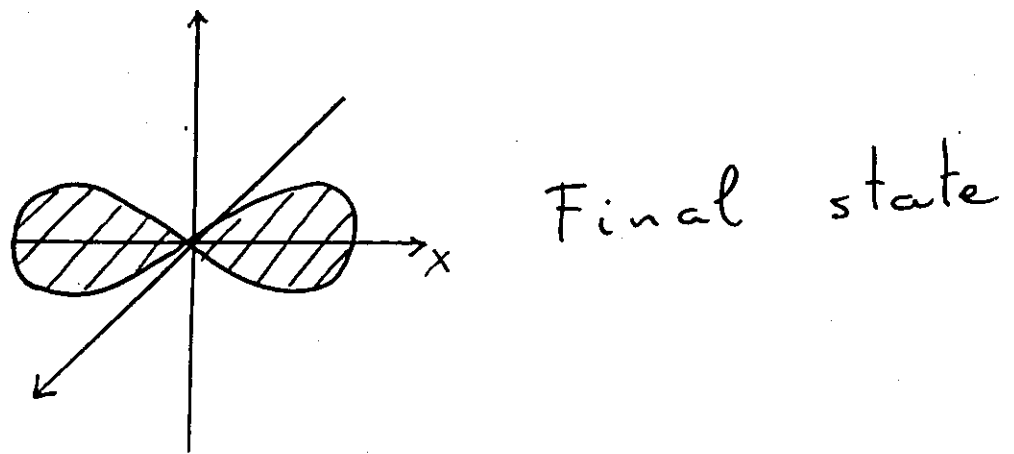
$$\int \psi_{i,\text{core}}^*(\vec{r}) \vec{A} \cdot \vec{p} \psi_f(\vec{r}) d\vec{r}$$

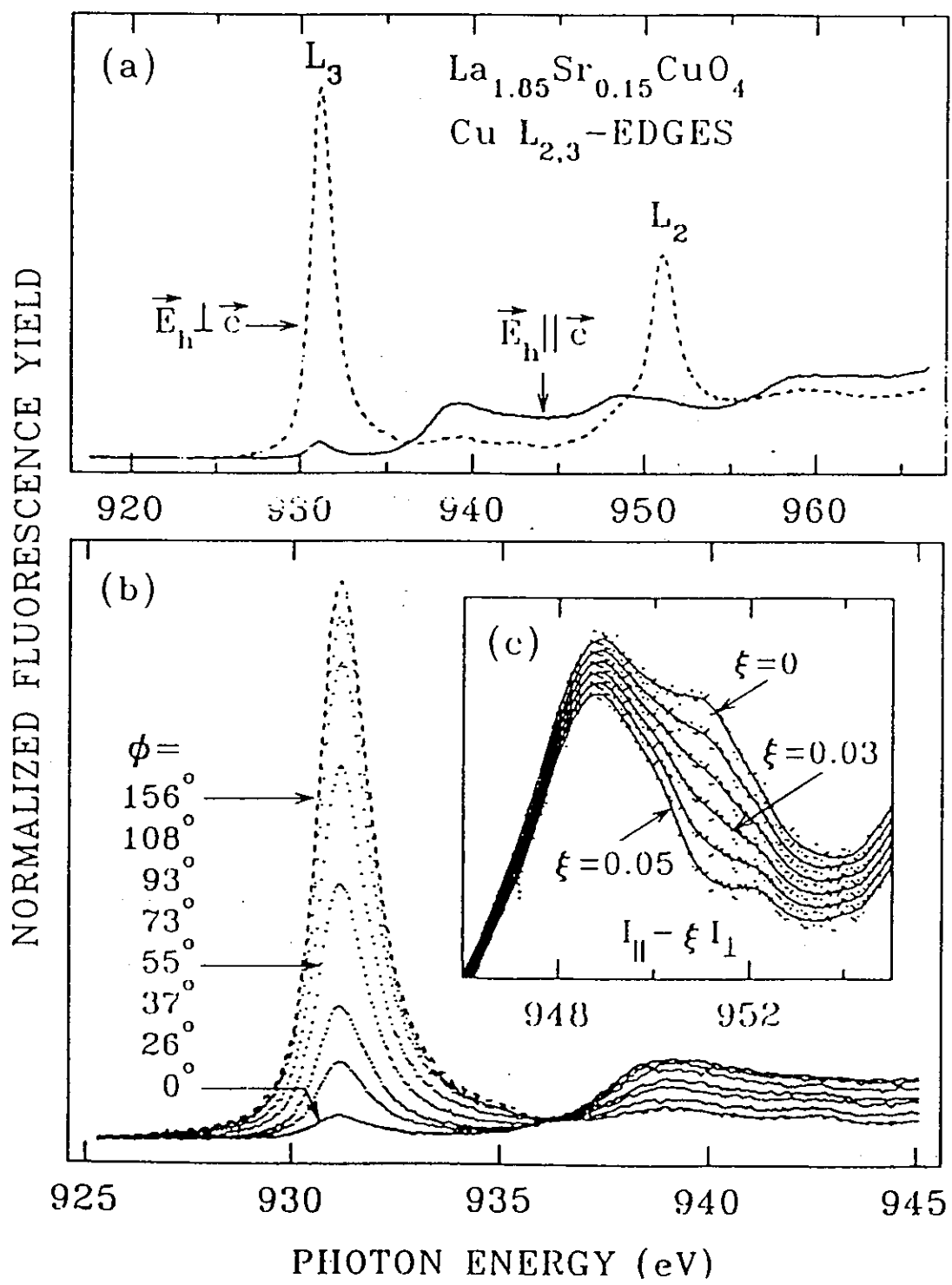
is a sensitive function of the amplitude of final wavefunction  $\psi_f(\vec{r})$  inside  $|\vec{r}| < r_c$  region.

Amplitude depends on interference of outgoing and reflected electron waves, with  $\lambda \sim \frac{\hbar}{\sqrt{2mE_{\text{kin}}}} = \frac{\hbar}{\sqrt{2m(E-E_{\text{th}})}}$

# Magnetic X-ray Dichroism







C. L. et al.  
 Phys. Rev. Lett. 75  
 152 (1995)

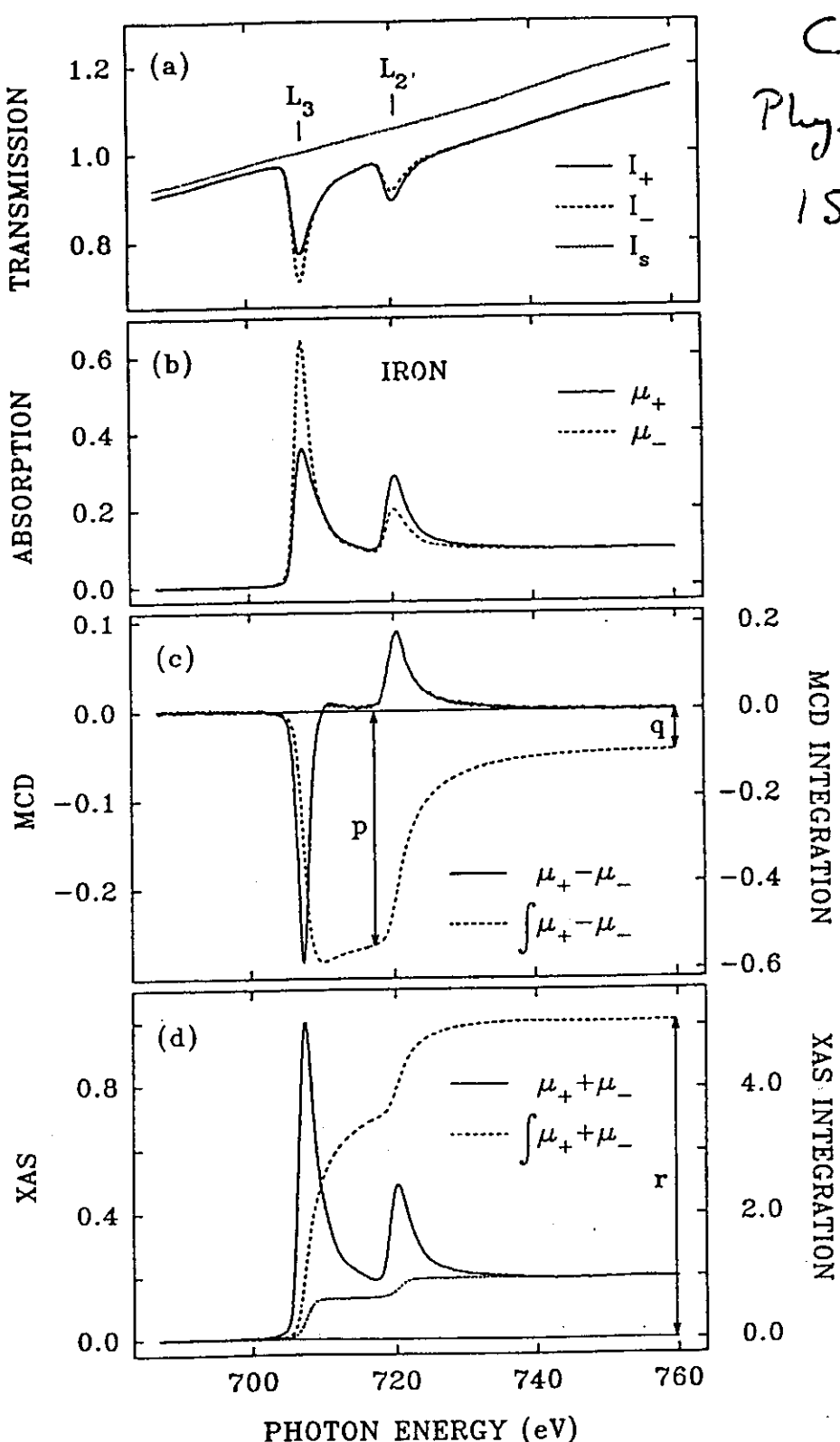


FIG. 1.  $L_{2,3}$ -edge XAS and MCD spectra of iron: (a) transmission spectra of Fe/parylene thin films, and of the parylene substrates alone, taken at two opposite saturation magnetizations; (b) the XAS absorption spectra calculated from the transmission data shown in (a); (c) and (d) are the MCD and summed XAS spectra and their integrations calculated from the spectra shown in (b). The dotted line shown in (d) is the two-step-like function for edge-jump removal before the integration. The  $p$  and  $q$  shown in (c) and the  $r$  shown in (d) are the three integrals needed in the sum-rule analysis.